INDONESIAN JOURNAL ON GEOSCIENCE
Geological Agency
Ministry of Energy and Mineral Resources

Journal homepage: https://ijog.geologi.esdm.go.id
ISSN 2355-9314, e-ISSN 2355-9306

Creep-Overpressure Coupling in The Onshore of Northeast Java Basin: Structural and Field-Based Geological Constraints

Eri S. Sitinjak[1*], Benyamin Sapiie[2], and Agus M. Ramdhan[2]

[1]Doctoral Programme in the Department of Geological Engineering, Faculty of Earth Sciences and Technology, Institut Teknologi Bandung, Jln. Ganesha, 10, Bandung, 40132, Indonesia
[2]Department of Geological Engineering, Faculty of Earth Sciences and Technology, Institut Teknologi Bandung, Jln. Ganesha, 10, Bandung, 40132, Indonesia

Corresponding author: erygea@yahoo.com or 32020003@mahasiswa.itb.ac.id
Manuscript received: May, 21, 2025; revised: November, 26, 2025;
approved: May, 11, 2026; available online: July, 24, 2026

Abstract - The onshore Northeast Java Basin is one of the most important oil and gas basins in Indonesia. The active Kendeng Fault plays a significant role in hydrocarbon generation and earthquake activity in the region. Studying the Kendeng Fault activity and its relationship with overpressure and earthquake potential could improve oil and gas exploration activities as well as natural disaster mitigation efforts in the onshore areas of the Northeast Java Basin. Therefore, this research focuses on surface geological mapping and laboratory analysis of field samples. Fault creep in the onshore of the Northeast Java Basin has not been studied continuously. Active mud volcanoes, which result from subsurface overpressure, may influence the creep rate and activity of Kendeng Fault segments. The Kendeng Fault meets the criteria of a creeping fault due to its geology, subsurface overpressure conditions, and geometry. Manifestations of creep near fault planes are clearly visible through geological phenomena such as landslides or physical changes in buildings. The Central Java morphology (Grobogan area) is rougher than The East Java morphology (Surabaya area), which suggests a possible difference in creep rate. The focal mechanism of recent earthquakes in the Kendeng Fault Zone indicates strike-slip or thrust faulting. The Central Java Fault segment exhibits a faster creep rate than the East Java Fault segment. This is evident through swarms of earthquakes at Gunung Pandan and Rawa Bening. Elemental analysis of the fluid and mud, combined with gas analysis of all the mud volcanoes in the studied area, shows a positive correlation between possible halide minerals (Na, Mg, Ca, K, and Cl) and gas content (N_2 and O_2/Ar). There is also a slight relationship between these gas and fluid elements (R^2). These parameters increase from the mud volcanoes in East Java to those in Central Java. CO_2 shows a negative correlation (r) and a slightly stronger relationship (R^2) with CH_4. The mud volcanoes in Central Java are dominated by CO_2, which may originate from volcanic activity in a deeper reservoir as a result of tectonic activity in the region. In contrast, the mud volcanoes in East Java are dominated by CH_4, which may originate from a highly overpressured hydrocarbon reservoir in a shallower area due to a high sedimentation rate. The very high sedimentation rate influences the slow-creeping fault segment in East Java (the Surabaya region) due to overpressure. Conversely, the faster creeping fault segment in Central Java (the Grobogan and Kesongo areas) may be influenced by volcanism due to tectonic activity in the region. These findings require further study, particularly the relationship of overpressure in each Kendeng Fault segment. The results will be useful for hydrocarbon exploration activities in the region as well as for natural disaster mitigation in general.

Keywords: fault creep, overpressure, mud volcano, earthquake, northeast Java Basin

How to cite this article:
Sitinjak, E.S., Sapiie, B., and Ramdhan A.M., 2026. Creep-Overpressure Coupling in The Onshore of Northeast Java Basin: Structural and Field-Based Geological Constraints. *Indonesian Journal on Geoscience*, 13 (2), p.269-296. DOI:10.17014/ ijog.13.2.269-296

Introduction

Background

Fault creep refers to the aseismic movement of a fault in the upper part of the earth crust during the interval between two earthquakes, releasing accumulated stress on the fault (Harris, 2017). This phenomenon can manifest as an after-slip event, occurring daily or annually following an earthquake (Cakir *et al*., 2012). Fault creep is controlled by at least three primary factors globally: the geological characteristics of the fault, the presence of overpressured fluids, and the geometry of the fault (Avouac, 2015; Chen and Bürgmann, 2017; Harris, 2017; Bürgmann, 2018). Research on fault creep began in the 1960s in the United States, focusing on the creeping movement of the San Andreas Fault, as observed through changes in physical infrastructure (Steinbrugge *et al.,* 1960). Changes such as shifts in buildings, roads, and outcrops were measured using simple creep meters-a practice that continues today with modernized instruments. Another example of fault creep includes the Chihshang Thrust Fault in Taiwan, which is known as the fastest creeping thrust fault globally, with an annual creep movement of approximately 2-3 cm (Lee *et al.,* 2003; Chen and Bürgmann, 2017).

Research on creeping faults has yet to be extensively conducted globally in many shallow continental faults. Fault creep in Indonesia, however, including the Kendeng Fault in East Java (Figure 1), where ~15% of the country's population resides, has yet to be well characterized. Most earthquake hypocentres on Java Island are located in its southern part (Santoso *et al.,* 2018). Since at least the 1770s, researchers have documented major earthquakes in the Central and East Java regions (Figure 1). The documented earthquakes have occurred onshore near the Kendeng Fault, which extends approximately 260 km from Semarang to Surabaya. The Kendeng Fault has

Figure 1. Map of documented major earthquakes on Java Island from 1815 to 1867, along with sample locations, water well blowout sites, and mud volcano (MV) locations. The model using DEM data was obtained from https://earthdata.nasa.gov/.

been dormant for a long period, and its activity is still under investigation. The fault, however, has become a priority for earthquake potential studies on Java Island (Lestari *et al.,* 2020). This research will be the first to focus on the creeping activity of the Kendeng Fault through surface geological observation.

The Kendeng Fault is situated within the Northeast Java Basin (Figure 1), where one of the massive mud volcano eruptions globally known as the Sidoarjo Mud Volcano or Lusi, occurred in 2006 (Miller and Mazzini, 2018). Following this phenomenon, smaller-scale blowouts were observed across the East and Central Java regions (Figure 1); most of these were associated with groundwater drilling to depths of ~200 m below the ground surface. The blowouts typically produced limited amounts of methane, mud, and water, which mostly ceased after a certain period. Given the generally tectonically active nature of Indonesia and the urgency of earthquake mitigation, it is vital to assess the creep of major faults in the country, including the Kendeng Fault. This study combines field observations and laboratory analysis to investigate the creeping behaviour of the Kendeng Fault and its relationship to overpressured conditions in the Northeast Java Basin.

Studied Area

The studied area is located in the onshore region of East Java, which can be divided into four zones (Figure 2) based on morphology, physiography, and major structural areas: The Rembang Zone in the northernmost part, The Kendeng Zone, The Modern Volcanic Arc, and The Southern Mountains (Bemmelen, 1949; Prasetyadi *et al.,* 2005). Structurally, the island of Java exhibits three dominant patterns: the northeast-southwest Meratus, east-west Java/Sakala, and north-south Sunda patterns. The Kendeng Fault is a thrust fault located across central and eastern Java with an east-west trend and correlates with the Java or Sakala structural pattern. The Kendeng Fault spans approximately 280-300 km with possible extensions into Central Java Province. This fault may also be connected to the Baribis Thrust Fault in West Java, creating a continuous fault system of approximately 800 km that extends from East Java to West Java (Koulali *et al.,* 2016).

The surface physiography reflects a lithological transition from the southern to the northern

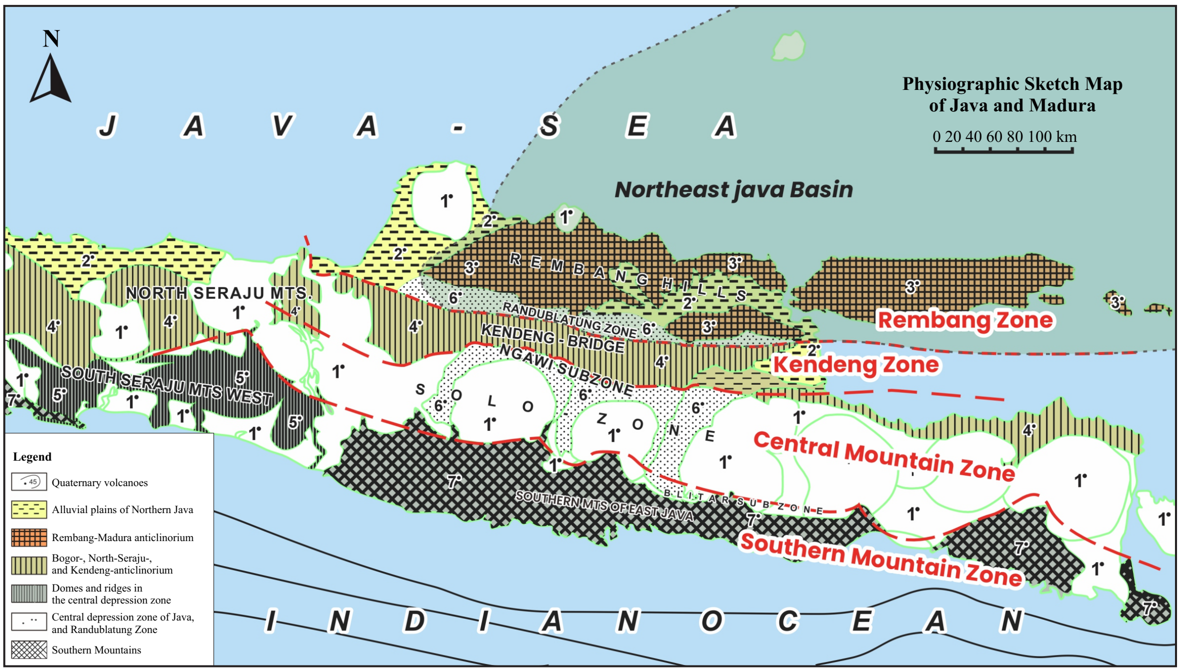

Figure 2. Physiography and major structural domains of East Java (modified from Bemmelen, 1949).

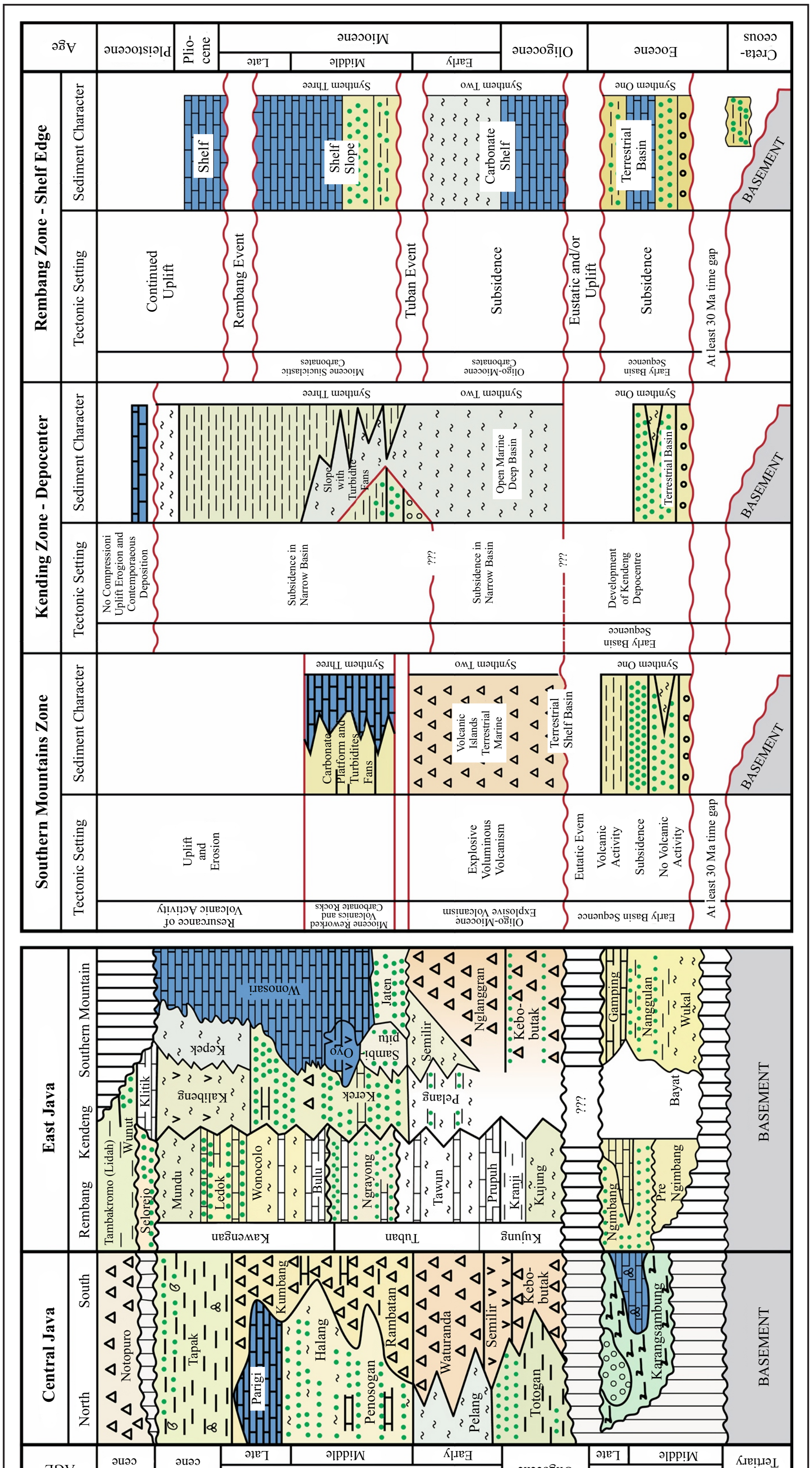

Figure 3. Regional stratigraphic column of Java Island (modified from Sribudiyani *et al*., 2003; Smyth *et al*., 2005).

part of Java. The southern part (Southern Mountain and Central Volcanic Mountain Zones) is dominated by volcanic rocks, whereas the Kendeng and Rembang Zones consist mainly of clay and sandstone, respectively (Julias *et al.,* 2017). Smyth *et al.* (2005) developed a comprehensive regional stratigraphic column (Figure 3) showing that the Kendeng Zone is primarily composed of clay and marl from the Kalibeng, Kerek, and Pelang Formations. Figure 3. Regional stratigraphic column of Java Island (modified from Sribudiyani *et al.,* 2003; Smyth *et al.,* 2005).

Burhannudinnur (2013) found that the source of mud in the mud volcanoes of the Rembang Zone is derived from Early Miocene to Mio-Pliocene sediments of the Tawun Formation. In contrast, the mud of the mud volcanoes in the Kendeng Zone is derived from Middle Miocene to Pliocene sediments of the Upper Kalibeng and Kerek Formations.

Methods

Geological field mapping was conducted, focusing on the suspected Kendeng Fault and mud volcano locations. Samples of rocks, water, mud, and gas were collected and carefully preserved for laboratory analysis. Rock samples were sent to the Geology Department of Institut Teknologi Bandung (ITB) for thin-section analysis. Water samples from mud volcanoes were analyzed at the Environmental Engineering Laboratory of ITB to determine the chemical composition. Muds from mud volcanoes were sampled for Scanning Electron Microscope (SEM) analysis at the Geological Survey Centre (PSG). The mud samples were also analyzed at the Soil Mechanics Laboratory of ITB for grain size and density analysis. Gas samples were analyzed at The Mineral Coal Centre and Geothermal Resources Laboratory to identify the chemistry.

Surface rupture observations were also carried out along the Kendeng Fault Zone to identify potential creeping activity. Observations focused on infrastructure within the fault zone, although detecting creep proved challenging due to the Kendeng Fault's slow creeping rate compared to other faster-moving faults globally. To address this limitation, this study integrates geological map data to constrain the locations of potential creeping activity. The results of the laboratory analysis were integrated with geological mapping to investigate the relationship between the creeping behaviour of the Kendeng Fault and overpressure conditions in the onshore Northeast Java Basin.

Result

Lithology

Field observations revealed that the Kendeng Zone (Figure 4) is primarily dominated by massive marl in the upper part, with marl interspersed with claystone, tuff, limestone, and sandstone in the lower parts of the Kerek (S30) and Kalibeng (S14) Formations (Pringgoprawiro, 1983).

The Sonde Formation (D2) is also present to the far east of the Kendeng Zone in the studied area (Figure 1), indicated by marl with sandstone and tuff interbeds (Pringgoprawiro, 1983). Thin-section analysis reveals that carbonate mud dominates the marl samples. Although classified as tuff lapilli, one sample (P5) shows that most lithic fragments and volcanic ash had already transformed into clay minerals.

At the A-2 location, the Kerek Formation consists of intercalated whitish marl, brown limestone, claystone, and blackish sandstone (Pringgoprawiro, 1983). The upper part of this formation is primarily composed of brown limestone, whereas the lower part is dominated by whitish marl. Minor faults and fracture zones were observed at the outcrop. Thin-section analysis classified the rock sample as sandy mudstone based on Dunham’s classification (1962). This is attributed to the predominance of very fine, darkish-brown carbonate mud with fragments of sandstone fragments containing plagioclase, alkaline feldspar, opaque minerals, and hornblende. The rock also contains planktonic foraminifera fossils.

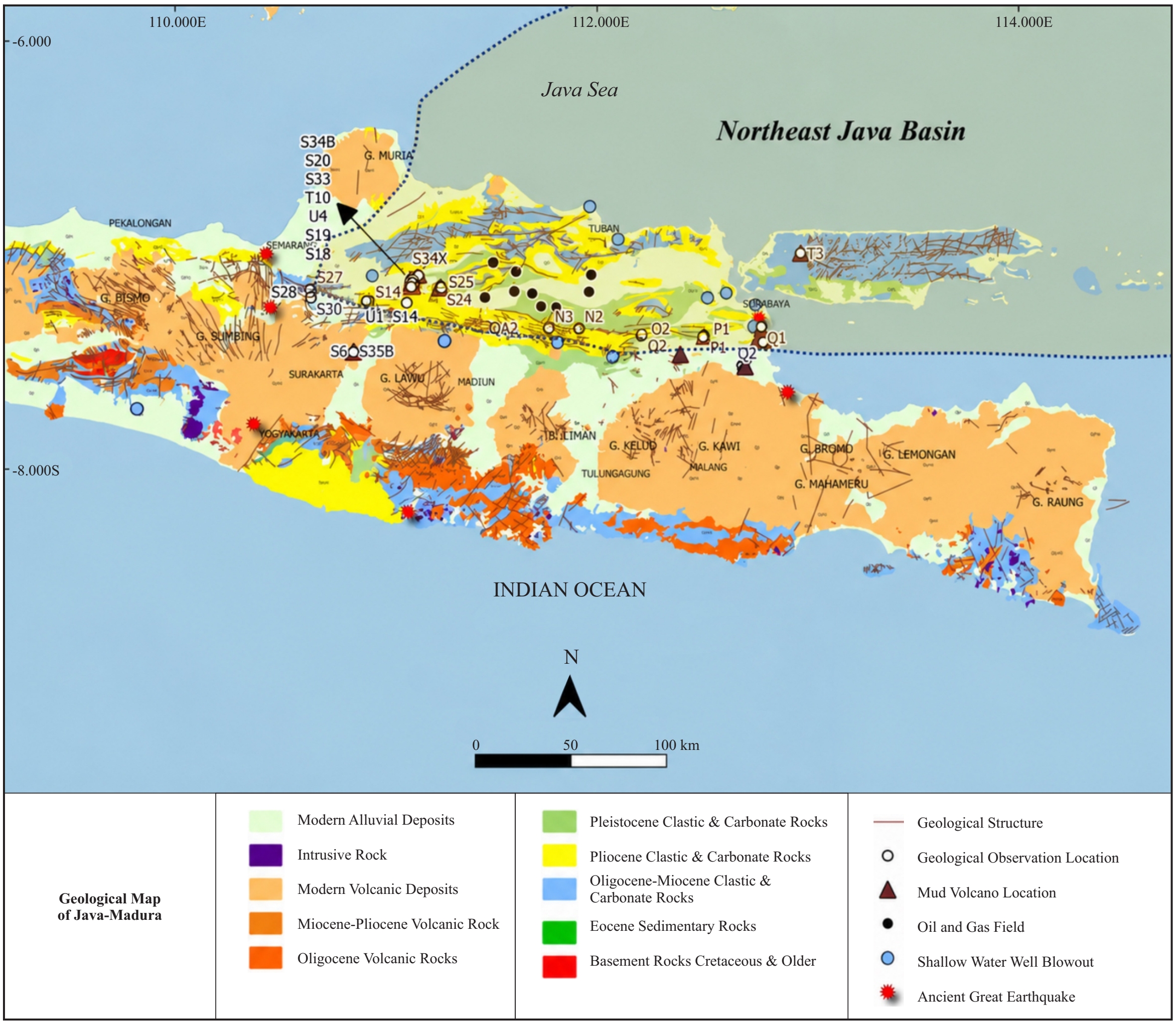

Figure 4. Simplified geological and structural map of the Northeast Java Basin (reproduced as the result of modification from Smyth *et al.* (2008), Gafoer and Ratman (1999), and Amin *et al.* (1999), showing the locations of rock samples, shallow water well blowout, and mud volcanoes from field investigations.

At the S14 location (Figure 5), the lithology is dominated by massive marl from the Kalibeng Formation. Poor road conditions were observed in this area, likely attributed to the lithology characteristics. Some sections experienced landslides which nearly severed the road entirely (Figure 5c). Approximately 100 m from the damaged road, small marl hills displayed high friability, making them prone to sliding. Thin section analysis classified the marl as Foraminiferal Mudstone (Dunham, 1962), characterized by very fine carbonate mud containing planktonic foraminiferal fossils. Some shells of these fossils had been replaced by micrites and opaque minerals.

At the P5 location, the Sonde Formation (Figure 6) was identified, accumulating within the Kedungwaru Anticline. The Sonde Formation consists of tuffaceous marl, yellowish-white in colour, containing diatoms and locally calcareous nodules (Pringgoprawiro, 1983). A minor reverse fault at P5 exhibited reverse motion, shifting the Sonde Formation (Figure 6). Macroscopic observations reveal that the tuff content dominates the lithology. Thin section analysis classified the lithology as tuff lapilli based on Fisher's classification (1966) in Figures 7a and 7b.

This pyroclastic rock comprises lithic fragments, crystal fragments, and lapilli-sized glass pieces embedded in a volcanic ash groundmass

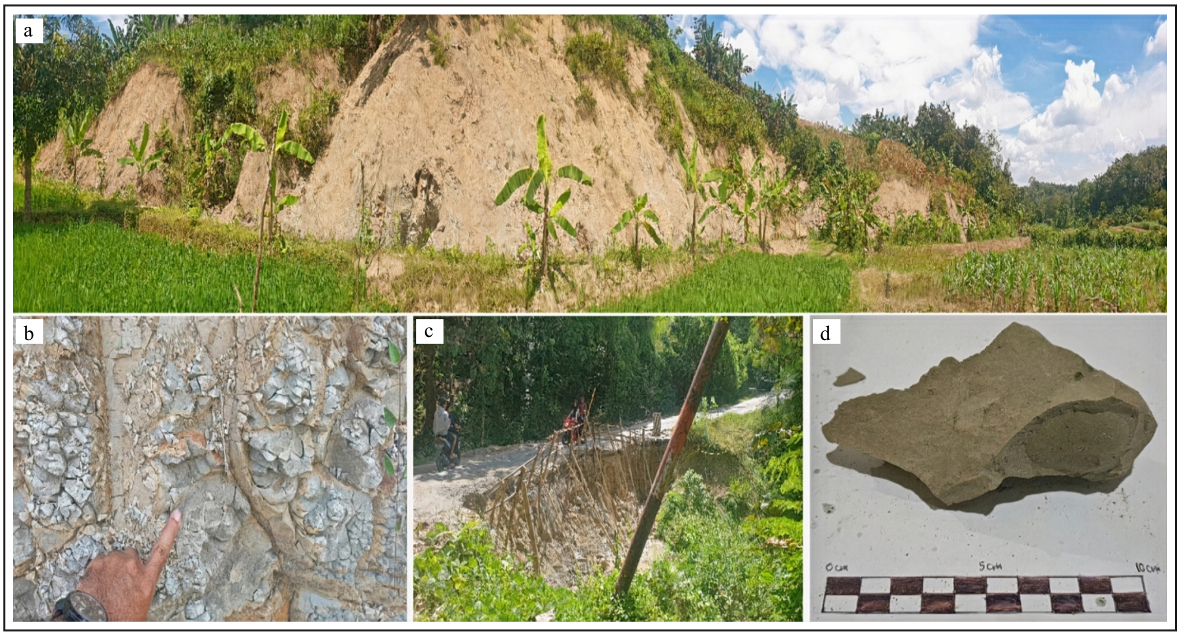

Figure 5. (a). Outcrop marl lithology from the Kalibeng Formation in S14 station; (b). Closer marl outcrop. from S14 station; (c). Indication of land movement or landslides close to S14 station; (d). Marl rock sample from S14 station.

Figure 6. Outcrop of the Sonde Formation in P5 station, along with a possible fault plane indicated by a purple dashed line (purple arrows are the possible fault movement). The red arrow indicates the fault plane lineament. The inserted photo is the close-up lithology of the site, dominated by tuffaceous marl.

(Figures 7a; b). The lithic fragments, primarily tuff, have largely transformed into clay minerals (Figures 7a; b). Crystal fragments include plagioclase and alkaline feldspar (Figures 7a; b), displaying microlite crystal forms (elongated, very fine, and white). Additional crystal fragments consist of mafic minerals and opaque minerals. The groundmass is composed of volcanic ash that has undergone alteration into clay minerals.

The U1 location is dominated by massive marl from the Kalibeng Formation. The marl is heavily fractured, likely due to structural deformation activities. Thin section analysis classified the rock as Foraminiferal Mudstone based on Dunham's

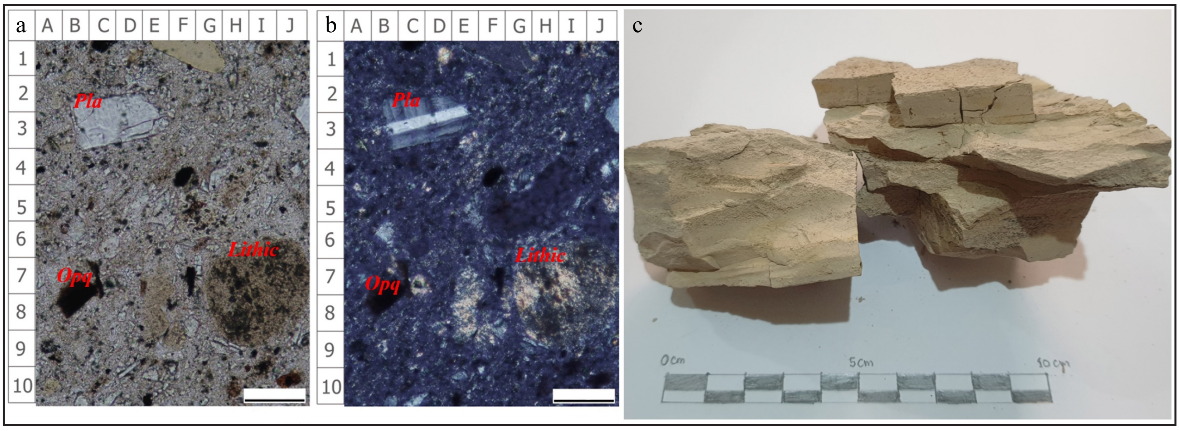

Figure 7. The Kalibeng Formation rock sample (c) from S14 station and thin section analysis: (a) parallel nicol. (b) and cross nicol. Some of the lithic fragments have changed to clay minerals. *Opq: Opaq mineral; Lithic: lithic fragment; Pla: plagioclase.*

classification (1962). The rock contains shells of planktonic foraminiferal fossils (Figures 8d and e) and opaque minerals.

The groundmass consists of micrites with a mud-supported fabric. Carbonate mud, identified by its darkish-brown colour and very fine grain size (micrite), is the dominant material exhibiting extreme birefringence. Fossil shells are less abundant than micrites, with skeletal grains primarily derived from planktonic foraminifera (Figure 9a). Some fossil shells are filled with rhombic dolomite crystals, along with calcite spars and possibly dolomite spars. Fine opaque minerals are present within some shell fossils (Figure 9a).

At the D2 location (Figure 8), the lithology comprises marl alternating with sandstone and tuff from the Sonde Formation (Figures 8a and 8b). This site features numerous fractures and minor faults due to its proximity to the Kendeng Fault. Thin section analysis classified the rock as Foraminiferal Mudstone (Dunham, 1962). Micrite carbonate mud, characterized by its darkish-brown colour and extreme birefringence, dominates the lithology, accompanied by shell fossils from planktonic foraminifera. The mud-supported fabric and dolomite-filled fossil voids were observed. Calcite and dolomite spar, identifiable by their rhombic crystal shapes, partially or fully replaced some fossil shells (Figures 8d and 8e). Opaque minerals, present as very fine grains or rounded aggregated crystals, filled foraminifera shell cavities (Figures 8d and 8e).

SEM analysis was performed to determine the mineralogy of carbonate mud or clay material. At S14 (Figure 9a), dominated by massive marl of the Kalibeng Formation, the clay and carbonate mud primarily consist of smectite, with some portions associated with illite. A similar mineralogical composition is found in the D2 sample (Figure 9b), where smectite dominated the clay minerals. Frequent occurrences of shell fossils and planktonic foraminifera fossils were observed across all samples. Smectite-illite, a phyllosilicate clay group, is identified as the primary mineral associated with the samples.

This mineral readily swells when interacting with water and is commonly associated with creeping faults, as it reduces the shear stress of faults, facilitating creep. Geological observations (Figure 4) indicate that the Kendeng Zone is predominantly composed of illite-smectite minerals, which may promote fault creep. Fractures and minor faults are common in areas near the Kendeng Fault, as depicted in the geological map.

Gas Composition

Gas samples collected from active mud volcanoes were grouped into three complexes based on their east-west distribution (Figure 10). The first group, the East Java Mud Volcano Complex, consists of the Surabaya and Madura Mud Vol-

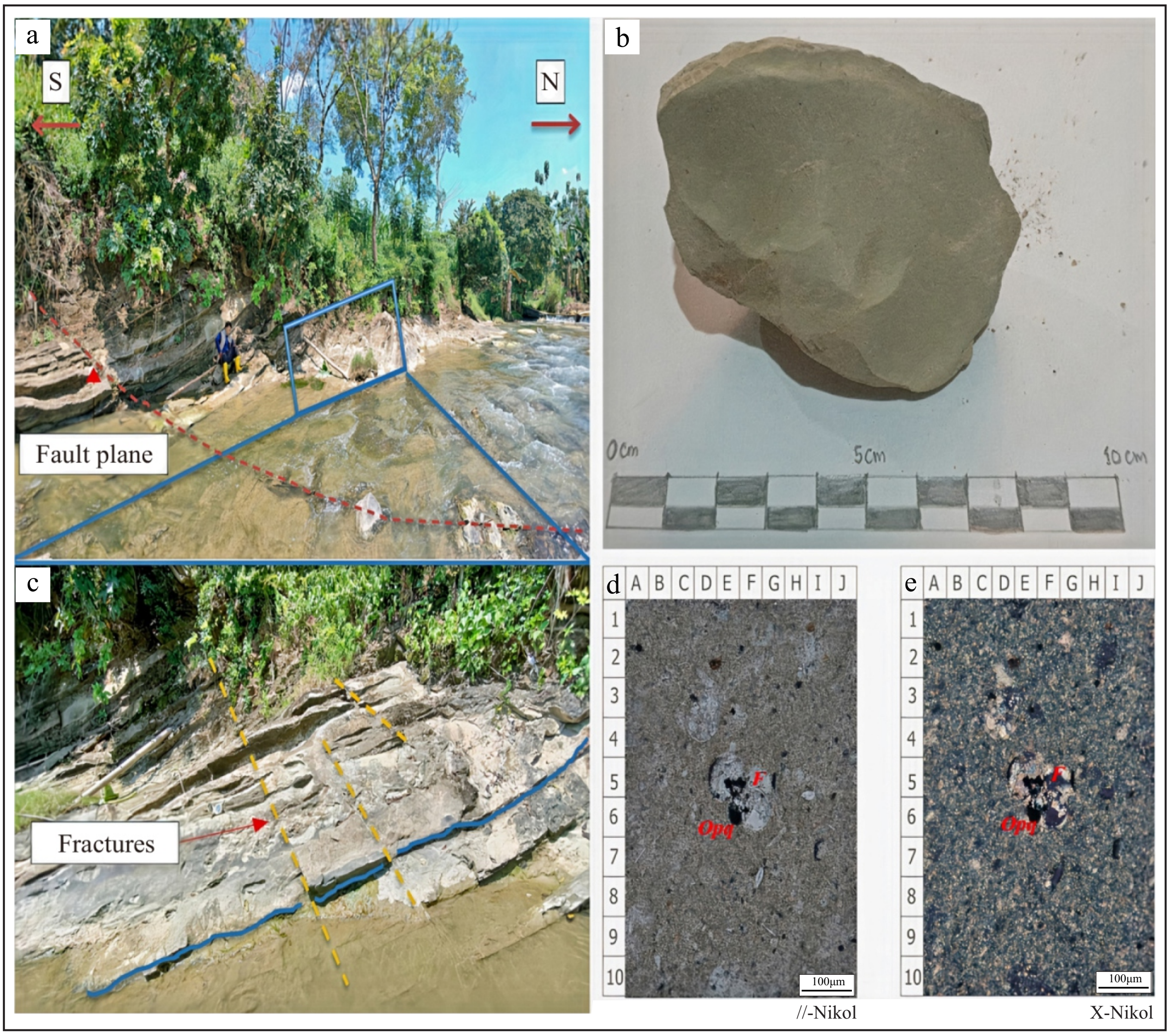

Figure 8. Outcrop of The Sonde Formation in D2 station, along with a possible fault plane (a); closer look of the D2 outcrop with fractures (b); marl rock sample from the D2 station (c); parallel nicols (d) and cross-nicol (e) thin section analysis of marl from D2 station. *F: foraminifera.*

cano Complex, including Soccah/Buhjel Tasek, Pulungan, Lusi, Banyu Mombol, Citro, Bekucuk, Gununganyar, Kalanganyar, and Wringinanom. The second group is the Central Java Mud Volcano Complex, which consists of the Kesongo Mud Volcano Complex (Kesongo, Anak Kesongo, and Banyu Geni Jati); the Grobogan Mud Volcano Complex (Medang, Buran Blegodah, Buran Londo Banjarejo, Bledug Detil, Bledug Kuwu, Cakringan, Crewek, Banjarlor, Little Volcano, and Detil); and The Sangiran Mud Volcano Complex (Sangiran and Pablengan). The third and westernmost group is the West Java Mud Volcano Complex, which consists of the Kuningan Mud Volcano or Ciuyah Mud Volcano.

The CO_2, O_2/Ar, and N_2 content in the gas samples increases from east to west, with the Surabaya Mud Volcano Complex having the lowest average CO_2 content (Table 1). Conversely, CH_4 content decreases along the same gradient, with the Surabaya Complex showing the highest CH_4 levels compared to the other complexes. This indicates that there is a significant difference between the mud volcano complex in Surabaya (Kendeng Zone) and the mud volcano in Grobogan, which represents the Rembang Zone. This trend indicates that subsurface CO_2, O_2/Ar, N_2 and CH_4 concentrations may be important factors influencing the creep behaviour of the Kendeng Fault, which may be

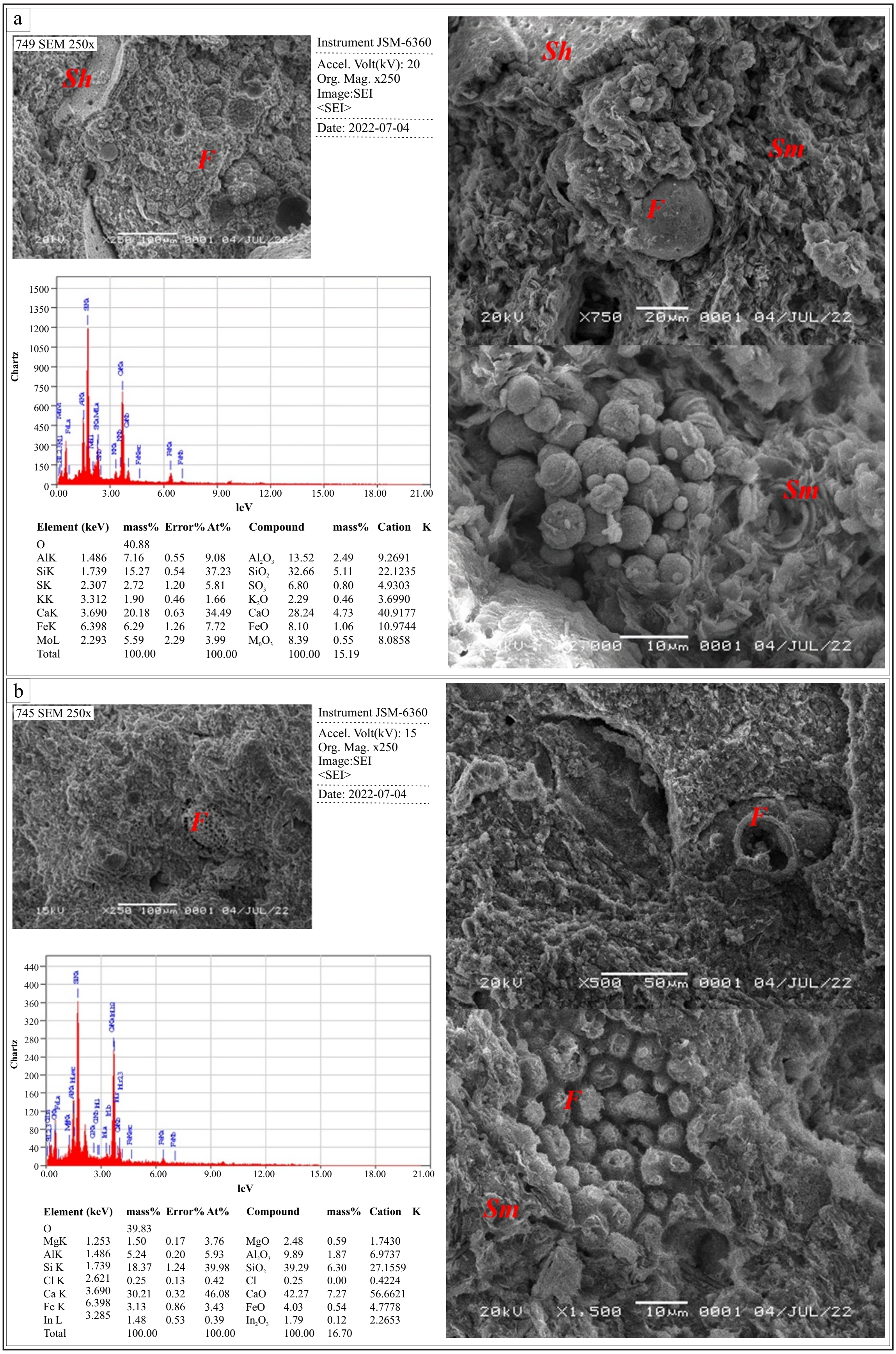

(a)

Element	(keV)	mass%	Error%	At%	Compound	mass%	Cation	K
O		40.88						
AlK	1.486	7.16	0.55	9.08	Al_2O_3	13.52	2.49	9.2691
SiK	1.739	15.27	0.54	37.23	SiO_2	32.66	5.11	22.1235
SK	2.307	2.72	1.20	5.81	SO_3	6.80	0.80	4.9303
KK	3.312	1.90	0.46	1.66	K_2O	2.29	0.46	3.6990
CaK	3.690	20.18	0.63	34.49	CaO	28.24	4.73	40.9177
FeK	6.398	6.29	1.26	7.72	FeO	8.10	1.06	10.9744
MoL	2.293	5.59	2.29	3.99	M_0O_3	8.39	0.55	8.0858
Total		100.00		100.00		100.00	15.19	

(b)

Element	(keV)	mass%	Error%	At%	Compound	mass%	Cation	K
O		39.83						
MgK	1.253	1.50	0.17	3.76	MgO	2.48	0.59	1.7430
AlK	1.486	5.24	0.20	5.93	Al_2O_3	9.89	1.87	6.9737
Si K	1.739	18.37	1.24	39.98	SiO_2	39.29	6.30	27.1559
Cl K	2.621	0.25	0.13	0.42	Cl	0.25	0.00	0.4224
Ca K	3.690	30.21	0.32	46.08	CaO	42.27	7.27	56.6621
Fe K	6.398	3.13	0.86	3.43	FeO	4.03	0.54	4.7778
In L	3.285	1.48	0.53	0.39	In_2O_3	1.79	0.12	2.2653
Total		100.00		100.00		100.00	16.70	

Figure 9. (a). SEM of S14 station rock sample; (b) SEM of D2 station rock sample. *F*: Foraminifera; *Sh*: Shell; *Sm*: Smectite.

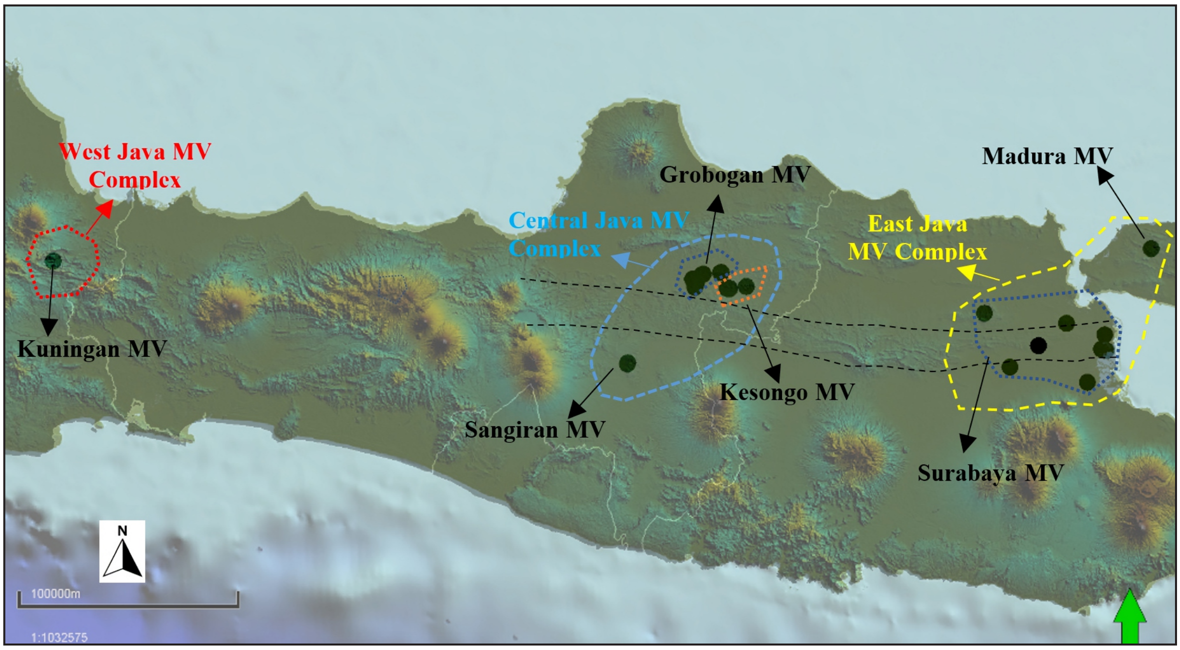

Figure 10. A map showing the distribution of mud volcanoes from Central to East Java. DEM data was taken from https://earthdata.nasa.gov/. MV: mud volcano.

Table 1. Gas Content of Mud Volcanoes in Java and Madura

Location	ID	Mud Volcano Complex	Parameters						
			Non-Condensable Gasses (%mmol)						
			CO_2	N_2	CH_4	O_2/Ar	He	H_2	CO
Buhjel Tasek/Soccah	T3	Surabaya and Madura	2.58	12.887	83.504	1.011	0.012	0.006	0
Gununganyar	Q1		12.58	13.56	72.318	1.542	0	0.001	0
Kalanganyar	Q2		3.64	18.02	76.258	2.069	0	0.013	0
Wringinanom	P1		6.39	15.19	77.242	1.158	0	0.004	0
Kesongo	S24	Kesongo	23.33	61.29	8.825	6.547	0.005	0.004	0
Anak Kesongo	S25		81.71	14.22	2.455	1.604	0.011	0.002	0
Crewek	S18	Grobogan	90.82	7.59	0.646	0.942	0	0	0
Banjarlor	S19		17.49	73.86	0	8.65	0	0.003	0
Bledug Kuwu	S20		81.71	14.22	2.455	1.604	0.011	0.002	0
Detil	T10		92.52	6.788	0.088	0.598	0.003	0.003	0
Cangkringan	S33		72.46	25.28	0.05	2.21	0.002	0	0
Medang-Pool	S34		95.71	2.26	1.841	0.183	0.004	0	0
Ciuyah	S37		82.43	15.06	0.651	1.86	0.002	0.003	0

related to volcanic activity and hydrocarbon generation in the region.

CO_2 indicates the influence of crustal magma, which represents a deep and high-temperature indicator. CO_2 content reduces fault friction and promotes faster creeping activity (Harris, 2017). Meanwhile, CH_4 indicates a shallower and lower-temperature environment, which is mostly related to hydrocarbon generation that creates an overpressure environment. However, the influence of CH_4 in reducing fault friction and promoting creeping activity is insignificant.

The creeping rate of the fault appears to increase from east to west, implying that the eastern segment of the Kendeng Fault (Surabaya) creeps more slowly than the western segment (Grobogan). This is based on the roughness of the morphology comparison between these two regions. The western part has a rougher surface morphology, represented by the mountainous areas, than the eastern part, represented by the alluvial plains. The observed increase in CO_2 content and decrease in CH_4 content from east to west align with this pattern. The Surabaya Mud Volcano Complex, with its higher CH_4 and lower CO_2 content, likely corresponds to slower creeping rates, whereas the western complexes exhibit conditions more conducive to faster creep, represented by a faster creeping rate. This may be related to the different nature of creeping activity in these two areas.

Mud and Water Analysis

Analysis revealed that the grain sizes in most mud volcanoes are dominated by clay and silt (Table 2), with specific gravity values ranging between 2.65 and 2.72. The clay and silt lithology are generally predominant in the mud sample. The inactive Sangiran mud volcano is unique in containing a small amount of gravel particles, which are absent in other active mud volcanoes. This is possibly due to interference with other sediments.

Table 3 shows the composition of the water samples. The main characteristic of water or fluids from the mud volcanoes in the studied area is its salinity. Elemental analysis of the fluid samples indicates that salt (NaCl) and magnesium contents increase from east to west (East Java Mud Volcano Complex to West Java Mud Volcano Complex, in Figure 9). In contrast, ferrum (Fe) or iron concentrations decrease along the same gradient (Table 3). The increase in magnesium content in Table 2 correlates with the increase in CO_2, O_2/Ar and N_2 content in Table 1 from east to west. Serpentine is the main mineral that promotes creeping activity in a fault zone, and magnesium is its main component. In general, higher magnesium content promotes faster creeping activity (Harris, 2017). Notably, the Kuningan Mud Volcano (Ciuyah), which is part of the West Java Mud Volcano Complex (Figure 9), exhibits significantly lower concentrations of strontium (Sr) and iron (Fe) compared

Table 2. Physical Properties of Mud Samples

No	Mud Volcano	ID	Gr	Sa	Si	Cl	% Finer by weight passing sleeve # 200	SG	GS	Lith
1	Sangiran 1	S 6	3	3	29	65	94	2.67	0.0040	Clay
2	Sangiran 2	S 35B	1	13	27	60	86	2.69	0.0053	Silt
3	Crewek	S 18	0	3	47	50	97	2.67	0.0102	Silt
4	Banjarlor	S 19	0	3	24	72	96	2.68	0.0021	Clay
5	Bledug Kuwu	S 20	0	3	20	77	97	2.69	0.0000	Clay
6	Kesongo	S 24	0	3	36	62	97	2.70	0.0046	Clay
7	Anak Kesongo	S 25	0	5	34	61	95	2.65	0.0047	Clay
8	Cakringan	S 33	0	4	23	72	96	2.68	0.0022	Clay
9	Medang	S 34	0	1	31	67	98	2.70	0.0034	Clay
10	Ciuyah	S 37	0	3	57	40	97	2.72	0.0105	Silt

Note:
SG: Specific Gravity GS: Grain Size No: Number Gr: gravel Sa: sand Si: silt Cl: clay Lith: lithology

Table 3. Fluid Content Analysis from Mud Volcanoes in Java and Madura

Location	ID	Mud Volcano Complex	Parameter Analysis (mg/L)										
			Cl	Na	K	Mg	Ca	SO_4	Sr	Li	Fe	B	pH
Gununganyar	Q1	Surabaya and Madura	14614	743	607	231	418	136	125	18.6	7332	0.001	7.77
Kalanganyar	Q2		15070	775	592	332	424	145	120	16.2	7219	0.001	7.52
Wringinanom	P1		16745	652	501	342	347	2.55	102	13.4	7426	0.001	7.33
Kesongo	S24	Kesongo	20094	4147	126.2	1104	210.6	238	34.69	6.06	0.001	0.001	7.81
Anak Kesongo	S25		19485	4743	175.6	708.7	298.9	510.4	39.17	0.96	0.05	0.001	7.86
Crewek	S18	Grobogan	31663	7213	2136	1263	672.6	187.1	62.86	23.01	3.46	0.001	7.29
Banjarlor	S19		25878	7209	1921	939.5	635.3	55.24	5.13	28.92	0.001	0.001	7.7
Bledug Kuwu	S20		74285	12908	4031	5335	2928	66.44	162.3	0.01	0.001	0.001	7.13
Cakringan	S33		32575	64S3	2122	1442	774.5	640.2	68.86	22.58	0.01	0.001	7.07
Medang	S34		20398	18.36	21.75	17.14	210.4	17.06	1.252	0.213	3.534	0.01	6.5
Detil	T10		36534	56.41	537.6	20.38	160.8	261	5.242	0.848	0.01	0.01	6.48
Sengon-Tuku	U4		27400	1201	38.72	62.74	149.8	7.64	98.77	30.15	0.03	0.001	6.53
Ciuyah	S37	Kuningan	16745	9556	1256	1427	557.1	143.8	2.13	8.69	0.07	0.001	6.72

to mud volcano complexes in the eastern region (Table 3).

The iron content in the East Java Complex is significantly higher than in the East Java Mud Volcano Complex. Iron appears in clay minerals such as illite, smectite, and chlorite. The transformation of smectite to illite can produce iron and magnesium. If released iron experiences oxidation in pore fluids, it will create coatings that cement grains, strengthen faults, and slow creep (Saffer *et al*., 2012; Ma *et al*., 2024). The presence of excessive iron will usually slow the creeping process, unless iron-bearing carbonates or sulphides dissolve and interact with deeper CO_2, which accelerates the creeping activity (Chiodini *et al.,* 2020).

Surface Rupture

Surface ruptures and minor landslides were observed on the sides of the Klubuk 1 bridge (O_2 station) and along nearby concrete drainage, as seen in Figure 11. This bridge was built over twenty years ago, and its location is close to a thrust fault, as indicated on the geological map. The area is part of the Kendeng Fault Zone, and is close to an active thrust fault. It is dominated by alluvium (Noya *et al*., 1992). The shifting of the concrete bridge and drainage, along with the landslide, indicate the movement history of this area over the last twenty years.

Nglambangan Village (N2 and N3 stations) is situated near the interpreted Ngrau Fault on the geological map. Signs of possible creeping include landslides and bumpy, wavy roads, suggesting physical changes due to fault activity. At Bago Village (S14 and S15 stations), massive marl from the Kalibeng Formation dominates the lithology (Figure 12).

The marl is loose, friable, and prone to interaction with water, contributing to deformation alongside fault activity. Fault escarpments and landslides are prevalent, and significant physical deformation of the area morphology has been observed. Poor road conditions may reflect fault movement or marl-water interactions.

Located near a suspected thrust fault on the geological map, the Gundih (U2 station) site is dominated by massive marl from the Kalibeng Formation. The station complex includes the Gundih train station, built in 1867, and the surrounding old buildings. Cracks that extend continuously in some buildings suggest creeping activity.

Intercalations of tuffaceous sandstone, calcareous siltstone, and marl from the Kalibeng Formation dominate the Kedungjati area (S27 and S28 stations in Figure 13 and Figure 4). At S27, east-west trending faults and fractures were observed in a nearby river. S28 is a railway station built in 1870, almost as old as the Gundih Train Station (Figure 13). Cracks in walls and significant deformation in the front porch floor were observed, suggesting creeping activity related to the Kendeng Fault.

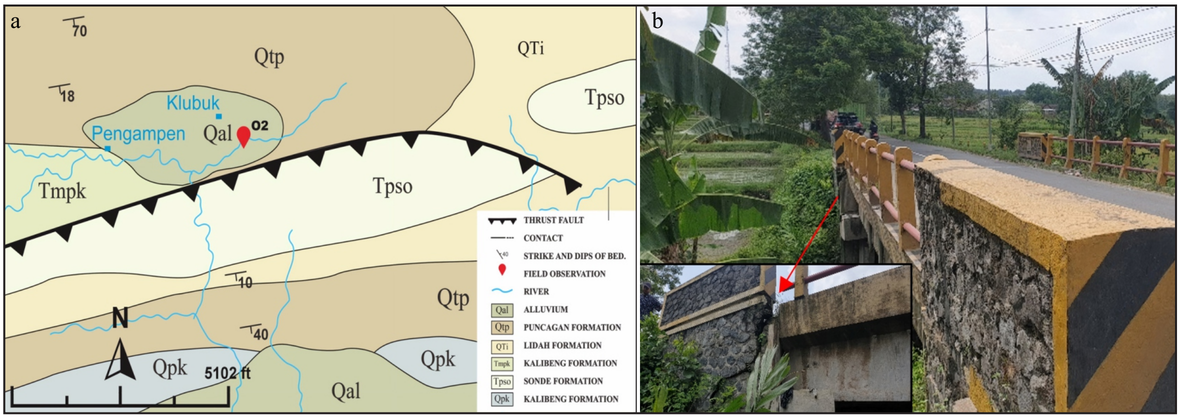

Figure 11. Possible indication of fault creep (displacement of the cemented wall bridge) at the O_2 station in the Klubuk 1 bridge (b); the location of the O_2 station on The Mojokerto Geological Map (Noya *et al.,* 1992); which clearly shows that the bridge is very close to a major thrust fault (a).

Figure 12. Manifestation of possible fault creep at N2 and N3 stations in the Nglambangan Village. N2 and N3 locations in The Bojonegoro Geological Map (Pringgoprawiro and Sukido, 2011) that close to the possible Kendeng Fault Zone (a), landslide at the N3 location (b), possible fault creep manifestation in N2 on the cemented road (s, d, and e).

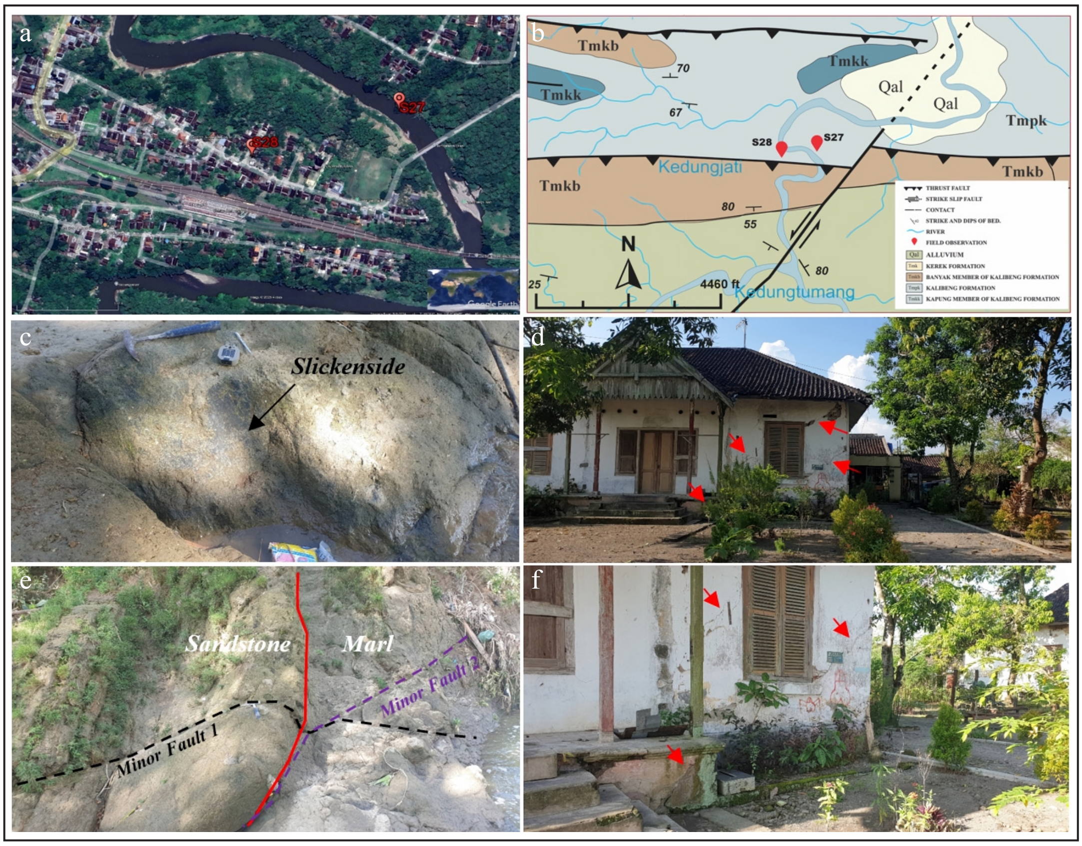

Figure 13. Possible creep manifestation at S27 and S28 stations in Kedungjati Village, image taken from Google Earth on March 3, 2025 (a); S27 and S28 in the Salatiga Geological Map (Sukardi and Budhitrisna, 1992), indicating how close these stations are to the major thrust fault (b); fault manifestation at S27 station (c, e), indicating some minor faults; slickenside (c) indicated an E-W direction of N260^{0}E with a plane dip of 3^0. Cracks on old buildings (red arrow) in S28 station (d, f), possibly indicating fault-creep manifestation. These old buildings were built by Dutch officials in 1870.

Discussion

Geological Characteristics and Fault Creep

The main result of this research is the outcome of geological field observations of creeping manifestations on the surface. Surface ruptures on old buildings and infrastructure were focused on that may have recorded the Kendeng Fault's creeping activity for decades. The focus was on the area where the interpretive fault is located on the geological map. In conclusion, Figures 10-13 provide compelling evidence of creeping activity in the Kendeng Fault Zone. Continuous observation is necessary to precisely define surface ruptures, as this researched area has never documented them before. Other observation methods are needed to determine the location of the surface rupture. This information will be useful when installing the fault creepmeter tool.

The geometry of a fault, including its length, the roughness of the surrounding morphology, and the creep rate, is another indication of creeping activity. Figure 13 shows a comparison of the geometry of the Kendeng Fault with that of the Alto Tiberina Normal Fault, the San Andreas Strike-Slip Fault, and the Chihsang Thrust Fault. These faults have the following creeping rates: The Alto Tiberina Normal Fault in Italy and the Chihsang Thrust Fault in Taiwan creep at 2-3 cm/year (Anderlini *et al.,* 2016; Gori *et al.,* 2018), while The San Andreas Strike-Slip Fault creeps at 3 cm/year (Rymer *et al*., 2006; Watt *et al*., 2014; Hirao *et al*., 2021). By comparison, the Kendeng Fault creeps at a rate of 3 mm/year (Koulali *et al*., 2016).

The lengths of the Alto Tiberina Normal Fault (Chiaraluce *et al*., 2014), the San Andreas Strike-Slip Fault (Steinbrugge *et al*., 1960), and the main Chihsang Thrust Fault are approximately 60 km (potentially extending to 100 km), 1,200 km, and 35 km, respectively. When combined with other faults in the Taiwan Longitudinal Valley, the Chihsang Thrust Fault system extends up to 160 km (Lee *et al*., 2003). The Kendeng Fault Zone extends about 260 km from Surabaya to Semarang, making it a major creeping fault. Figure 14 clearly shows the roughness of the well-known creeping faults around the world in each A-B cross-section. The Alto Tiberina, San Andreas, and Chihshang Faults have the average elevation differences of 1,500-3,500 feet, 1,500-2,500 feet, and 1,500-3,000 feet, respectively. The Kendeng Fault has the least elevation difference on average at around 20-600 feet. This correlates with the creeping rate of each fault, with the Kendeng Fault having the lowest rate (Figure 14).

Another piece of evidence of creeping faults is the presence of mud volcanoes, which may have different creeping rates than other fault segments. In Central Italy, where the Alto Tiberina Fault is located, several mud volcanoes exist, including the mud volcano at Pieve Santo Stefano near Mount Fungaia, which is situated at the northern end of the fault. Mud vents on the San Andreas Fault are located near its southern end in Palm Springs, close to the Salton Lake area. This area is considered the southern fault extension into Mexico. This segment creeps at a slower rate than the central and northern segments. Most earthquake activity occurs in the central and northern segments of the fault (Jolivet *et al.,* 2015; Kim *et al.,* 2016; Scott *et al.,* 2020). Several papers have already demonstrated the relationship between fault activity and overpressure buildup in the region, which caused intermittent creeping (Tong *et al.,* 2013; Khoshmanesh and Shirzaei, 2018; Xu *et al.,* 2018; Xu *et al.,* 2021). Preliminary observations suggest that the fault's lower creeping rate may be associated with mud volcano activity in the area (Xu *et al.,* 2018; Marshall *et al.,* 2024).

Studies of the San Andreas Fault have shown that reactions between serpentinite and hydrothermal, silica-rich fluids produce talc, reducing the shear strength of the surrounding rocks. This process contributes to the San Andreas Fault's stable creeping behaviour (Moore and Rymer, 2007). Similarly, other phyllosilicate minerals abundant in clay-rich rocks (*e.g*., montmorillonite, smectite, and illite) can reduce shear stress along faults. Water-saturated smectite, for example, exhibits frictional strength comparable to talc at room temperature.

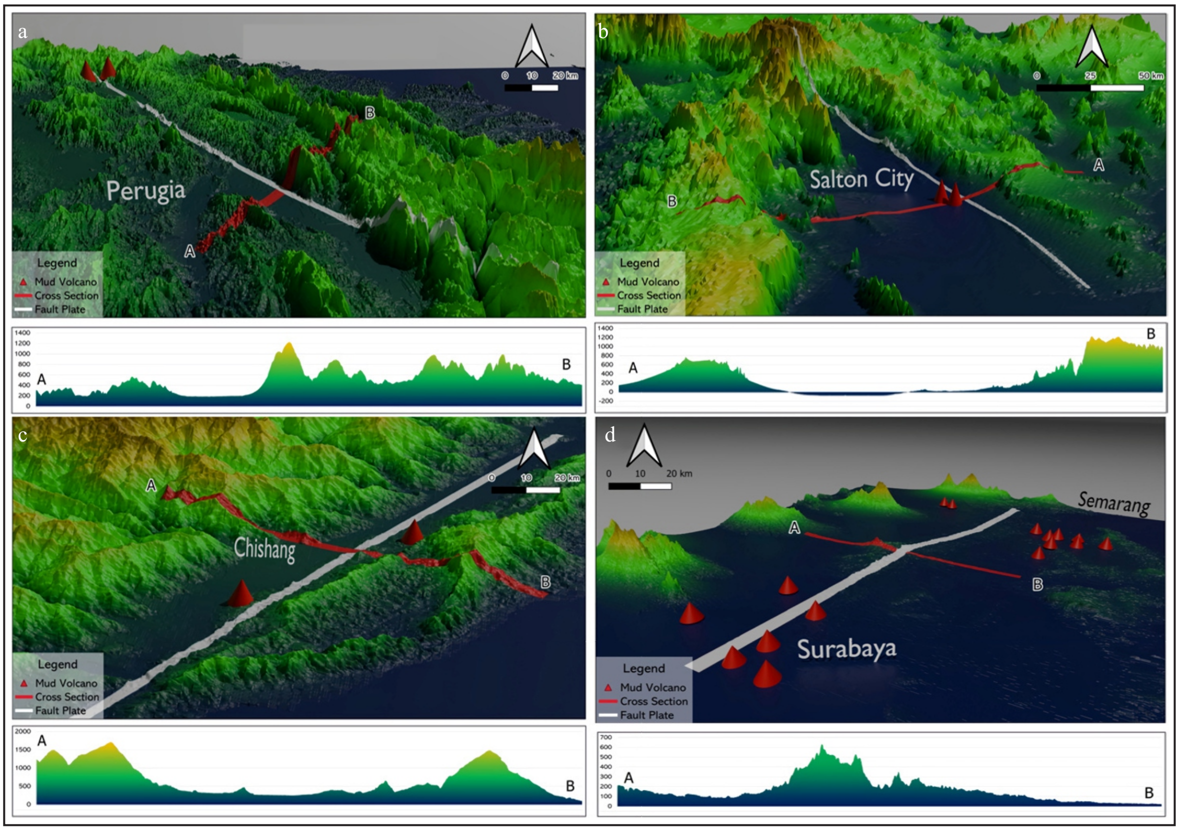

Figure 14. Average roughness of Alto Tiberina (a), San Andreas (b), Chihshang (c), and Kendeng Faults (d) from DEM modelling (DEM data was taken from https://earthdata.nasa.gov/).

Subsurface fluids also play a critical role in fault behaviour. For example, the interaction of ultramafic rocks with silica-rich hydrothermal fluids can produce talc on serpentinite at high temperatures. At lower temperatures, these processes produce clay and other phyllosilicate minerals. The Kendeng Fault Zone is dominated by marl in mud. According to SEM analysis, the mud contains smectite or illite, which are phyllosilicate minerals that can contribute to creep activity (Figure 9).

The Chihshang Fault has two mud volcanoes on its coastal side, the Lei Gong Huo and the Luoshan. In contrast, the Kendeng Fault has a higher number of mud volcano manifestations, including the massive Lusi Mud Volcano. However, the role of mud volcanoes in influencing the creeping movement of the Kendeng Fault remains unclear. Figure 15 summarizes all the mud volcanoes visited in the region (Sitinjak and Harbowo, 2024). The presence of mud volcanoes indicates overpressure conditions in the subsurface. This overpressure may be related to differences in the creep rate of nearby fault segments.

The last piece of evidence possessed by the Kendeng Fault indicating creeping activity is the occurrence of swarm earthquakes (seismicity). The focal mechanism of the recent ~10 km earthquakes in the Kendeng Fault Zone linearity suggests that the fault mechanism involved is a strike-slip to thrust fault mechanism (Figure 16). These focal mechanisms are located from the far east offshore Situbondo, Gunung Pandan, Rawa Bening, to Kali Bening in the far west. Gunung Pandan and Rawa Bening, located at the Kendeng Fault Zone, are noted for their very interesting local swarm earthquakes. Swarm earthquakes consist of a series of small earthquakes that occur over a short period of time without any dominant main shocks. They are also an indication of fault creep in an active tectonic region. This swarm of earthquakes confirms that the western part of

Figure 15. Active mud volcanoes in the onshore Northeast Java Basin and its sampling activity. The location of the mud volcanoes is depicted in Figure 1 (modified from Sitinjak and Harbowo, 2024).

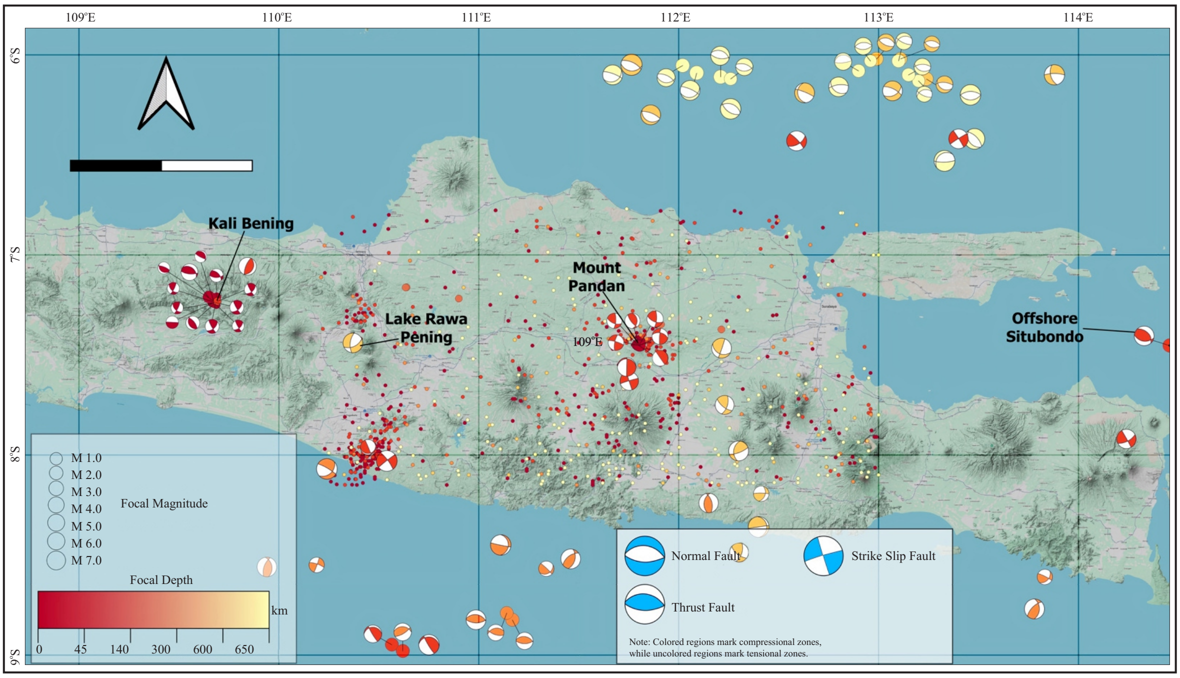

Figure 16. Focal mechanism of recent ~10 km deep earthquakes in East Java and Central Java (Source: https://www.isc.ac.uk/iscbulletin/search/fmechanisms/interactive/).

the Kendeng Fault Zone (Grobogan) is more active than the eastern part (Surabaya). Santoso *et al*. (2018) summarise a swarm of earthquakes in Gunung Pandan that were due to tectonic activity related to the Kendeng Thrust Fault. A low-density body under Gunung Pandan, as indicated by the residual gravity anomaly, dips to the south and is suspected to be related to a hot material or magma source. Further investigation of these two locations (Gunung Pandan and Rawa Bening) is needed to understand the creeping activity of the Kendeng Fault. Seismicity in Alto Tiberina was suspected due to overpressure, which also correlates with the anomalous flux of regional CO_2 in Central Italy (Chiaraluce *et al.,* 2014; Rainone *et al.,* 2015; Blumetti *et al.,* 2017; Agostinetti *et* *al.,* 2017; Valoroso *et al.,* 2017; Essing and Poli 2022). Gunung Pandan and Rawa Bening are perhaps the best places to assess fault creep. This study also concluded that the Kendeng Thrust Fault is an active creeping fault, similar to other creeping faults around the world. However, the rate of movement may differ among its segments.

Overpressure Conditions and Fault Creep

Overpressure in the Northeast Java Basin is not new (Ramdhan *et al.,* 2013; Burhannudinnur, 2013; Sitinjak, 2016; Sitinjak *et al*., 2017; Sitinjak, 2018). Overpressure conditions in the subsurface may contribute to fault creeping by reducing the effective normal stress acting on the fault. This phenomenon has been extensively documented, particularly in hydraulic fracturing studies (Sibson, 2014; Schultz *et al.,* 2020; Hadizadeh *et al.,* 2024). Wei *et al.* (2009) suggested that fault creep along the Superstition Hills Fault in California-equivalent to a magnitude 4.7 earthquake in 2006-could be attributed to elevated pore pressure in the sediments.

Laboratory experiments conducted by Ougier-Simonin and Zhu (2013) on intact porous sandstone samples at room temperature revealed that increased pore pressure could lead to brittle deformation, causing rocks to fail at lower shear strengths even within the brittle regime. One of the best-documented examples of fault creeping is the Chihshang Fault in the Longitudinal Valley, Taiwan (Chen and Bürgmann, 2017). This fault, a thrust fault similar to the Kendeng Fault, creeps at a rate of 20-30 mm/year, making it the fastest-creeping continental reverse fault in the world. Its manifestation can be observed along the longitudinal valley road, where a creep meter tool has been installed since 1998. Lithology and pressure solution creep are believed to play crucial roles in the creeping behaviour of the Chihshang Fault (Chao *et al.,* 2013; Thomas *et al.,* 2014; Chen *et al.,* 2020; Chao *et al.,* 2021; Franklin and Huang, 2022; Chao, 2023; Lee *et al.,* 2023). Mud volcano manifestations are also present along some parts of the fault. The onshore of the North-East Java Basin is a warm or hot and overpressure basin formed by rapid sedimentation in the Kendeng Zone (Mazzini *et al.,* 2012; Sitinjak, 2016; Putriyana *et al.,* 2023). Since the Lusi Mud Volcano incident, numerous studies have focused on overpressure conditions in the region. These investigations consistently highlight the overpressure subsurface conditions within the basin, where the Kendeng Fault is located. Overpressure conditions are evidenced by the manifestation of mud volcanoes at the surface (Baloglanov *et al.,* 2018). Several incidents of water drilling in the onshore of the North-East Java Basin have caused significant, albeit temporary, fluid or gas blowouts, indicative of overpressure conditions (Humaida *et al.,* 2012; Zaennudin *et al.,* 2013; Harianto, 2018; Rofiq, 2021). Throughout Java and Madura Islands, at least eighteen active and inactive mud volcanoes have been visited and identified in this research. However, not all mud volcanoes have sufficient data.

Gratier *et al.* (1999) highlighted the significance of pressure-solution creep in fault creeping. Pressure solution creep involves stress-driven mass transfer processes, including plasticity, fracturing, and electrochemical interactions. It serves as a primary mechanism for ductile deformation in the upper crust, facilitating basin compaction, folding, shear zone development, fault creep, and inter-seismic activity. Elevated fluid pressure can reduce the frictional resistance of faults, enhancing sliding potential (Scholz, 2019).

Based on the analysis of liquid and gas contents in Tables 1 and 2, a quantitative analysis was performed to determine the correlation and relationship among the measured parameters. It is done by defining the correlation co-efficient (r) and determination co-efficient (R^2) in a matrix table. Based on the calculation of the fluid parameters, Mg, K, Na, Ca, and Cl have a closed relationship with each other, giving a correlation co-efficient (r) range between 0.63-0.89 (Cl and Na provide the lowest r value of 0.63, and Mg-Ca, K-Ca together with Cl-Ca give the highest r value of 0.89). Meanwhile, the co-efficient of determination (R^2) gives a range of 0.39 to 0.93 (Cl and Na give the lowest R^2 value of 0.39, and Mg-Ca provide the highest R^2 value of 0.93). It seems that among the fluid parameters, Mg-Ca has the strongest relationship, while Na-Cl gives the lowest relationship (Figure 17c), which may be related to the nature of halide mineral dominance.

The parameters Mg, K, Na, Ca, and Cl (from fluid sample) have a positive correlation with N_2 and O_2/Ar (from gas sample) as depicted in Figure 17d, but the co-efficient of determination (R^2) varies from 0.22 to 0.59. The strongest relationship (R^2) was found from Mg and Ca (from liquid sample) to N_2 and O_2/Ar (from gas sample), giving an R^2 value of 0.49-0.59. Mg, Ca, N_2, and O_2/Ar are the indication of volcanic influence in the mud volcanoes, and the trend of this fluid and gas is increasing from Surabaya Mud Volcanoes to Grobogan and Kesongo Mud Volcanoes. Surabaya Mud Volcanoes have the lower Mg, Ca, N_2, and O_2/Ar content. This is an indication that the Grobogan and Kesongo Mud Volcanoes are strongly influenced by volcanic activity, unlike the Surabaya Mud Volcano Complex.

The gas parameters were calculated and surprisingly showed only two pairs of parameters that exhibited a relationship or association (Table 4). They are CO_2 and CH_4 that provide a correlation co-efficient (r) of -0.80, indicating a negative correlation with each other (Figures 17a and 17b). Secondly, N_2 - O_2/Ar provides a correlation co-efficient (r) of 0.99, which means a positive correlation with each other.

These strong correlations are also reflected in the value of the co-efficient of determination (R^2), which is 0.64 for CO_2 - CH_4 and 0.99 for N_2 - O_2/Ar. CO_2 was dominated in the Central Java Mud Volcano Complex, while CH4 was dominated in the East Java Mud Volcano Complex. CO_2 and CH_4 are negatively correlated and also related to each other. High CO_2 concentration can be suspected as an indicator of volcanic influence, indicating deeper reservoir influence (deep magmatic reservoir), while CH_4 is mainly a product of biogenic processes or perhaps related to hydrocarbon generation that is at shallower depth (Cabassi *et al.,* 2013; Navarro *et al.*, 2022).

This finding is consistent with Burhannudinnur (2013) that the mud volcanoes in the Central Java Mud Volcano Complex (Grobogan or Rembang Zone) are related to the Tawun Formation (Early Pliocene). This formation is much deeper than the source of the East Java Mud Volcano Complex (Surabaya or the Kendeng Zone), which is related to the Upper Kalibeng or the Kerek Formation (Middle Miocene to Pliocene). The East Java Mud

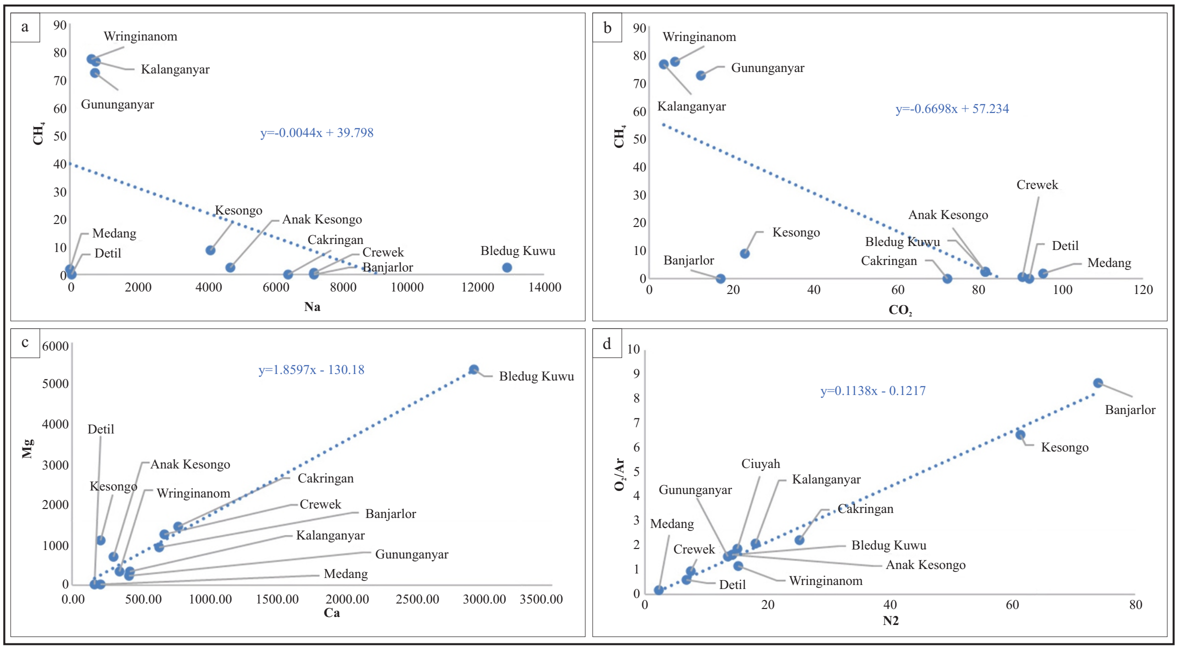

Figure 17. Negative and positive correlation graphs among fluid and gas parameters.

Table 4. Matrix Table of the Correlation Coefficient (r) on the Top and the Coefficient of Determination (R^2) on the Bottom, for The Respective Parameters of Liquid and Gas Analysis

r	Cl	Na	K	Mg	Ca	SO_4	Sr	Li	Fe	B	pH	CO_2	N_2	CH_4	O_2/Ar	He	H_2
Cl	-	0,63	0,83	0,87	0,89	-0,01	0,37	-0,26	-0,42	0,04	-0,25	0,07	0,60	-0,48	0,64	-0,11	-0,18
Na		-	0,83	0,85	0,75	0,09	0,13	0,07	-0,54	-0,50	0,03	0,14	0,55	-0,52	0,60	-0,07	-0,26
K			-	0,87	0,89	-0,03	0,42	0,22	-0,31	-0,35	-0,08	0,14	0,47	-0,47	0,52	0,05	-0,22
Mg				-	0,89	-0,03	0,42	0,22	-0,31	-0,35	-0,08	-0,15	0,73	-0,32	0,77	-0,18	-0,11
Ca					-	-0,14	0,59	-0,14	-0,19	-0,28	-0,05	-0,16	0,70	-0,30	0,75	-0,15	-0,10
SO_4						-	-0,12	0,03	-0,33	-0,15	0,13	0,10	0,18	-0,23	0,15	0,47	-0,15
Sr							-	0,09	0,59	-0,48	0,34	-0,71	0,48	0,46	0,48	0,09	0,36
Li								-	0,26	-0,51	0,38	0,14	-0,44	0,14	-0,42	0,36	-0,07
Fe									-	-0,26	0,33	-0,64	-0,17	0,81	-0,18	0,00	0,57
B										-	-0,73	0,52	-0,35	-0,33	-0,35	-0,05	-0,26
pH											-	-0,66	0,26	0,55	0,21	0,03	0,21
CO_2												-	-0,44	-0,80	-0,40	0,19	-0,59
N2													-	-0,19	1,00	-0,16	0,12
CH4														-	-0,23	-0,10	0,57
O_2/Ar															-	-0,18	0,10
He																-	-0,07
H_2																	-

x	Cl	Na	K	Mg	Ca	SO_4	Sr	Li	Fe	B	pH	CO_2	N_2	CH_4	O_2/Ar	He	H_2
Cl	-	0,39	0,69	0,75	0,80	0,00	0,14	0,07	0,18	0,00	0,06	0,00	0,36	0,23	0,41	0,01	0,03
Na		-	0,69	0,72	0,56	0,01	0,02	0,01	0,29	0,25	0,00	0,02	0,31	0,27	0,36	0,00	0,07
K			-	0,75	0,80	0,00	0,18	0,05	0,09	0,12	0,01	0,02	0,22	0,22	0,28	0,00	0,05
Mg				-	0,93	0,00	0,23	0,03	0,11	0,12	0,00	0,02	0,53	0,10	0,59	0,03	0,01
Ca					-	0,02	0,35	0,02	0,04	0,08	0,00	0,02	0,49	0,09	0,56	0,02	0,01
SO_4						-	0,01	0,00	0,11	0,02	0,02	0,01	0,03	0,05	0,02	0,22	0,02
Sr							-	0,01	0,35	0,23	0,12	0,51	0,23	0,21	0,23	0,01	0,13
Li								-	0,07	0,26	0,15	0,02	0,19	0,02	0,17	0,13	0,00
Fe									-	0,07	0,11	0,41	0,03	0,66	0,03	0,00	0,33
B										-	0,53	0,27	0,12	0,11	0,12	0,00	0,07
pH											-	0,43	0,07	0,30	0,04	0,00	0,04
CO_2												-	0,19	0,64	0,16	0,04	0,35
N2													-	0,03	0,99	0,03	0,01
CH4														-	0,05	0,01	0,32
O_2/Ar															-	0,03	0,01
He																-	0,01
H_2																	-

Volcano Complex appears to be more influenced by biogenic processes related to hydrocarbon and overpressure generation. Sedimentation rates also differ between East Java and Central Java.

The sedimentation rate in East Java is much higher, about 1,000-1,200 m/million years, while the sedimentation rate in Central Java ranges from less than 100 m/million years to 700 m/million years (Burhannudinnur, 2013). This also indicates that overpressure due to rapid sedimentation plays a more dominant role in East Java than in Central Java. Thus, the creep activity in the Kendeng Fault is influenced by two factors: Central Java is more affected by volcanic or tectonic activity, whereas East Java is more affected by overpressure due to a high sedimentation rate. The correlation co-efficient (r) and the determination (R^2) co-efficient are summarized in Table 4.

The increase of CO_2 followed by a decrease of Fe will reduce the pH and Sr from the East Java Mud Volcano Complex to the Central Java Mud Volcano Complex. Increased dissolved magnesium in calcite strengthens the transition between diffusion and dislocation creep (Herwegh *et al.,* 2003). Furthermore, magnesium in phyllosilicate minerals contributes to reducing a fault's frictional strength. Fine grains within the fault accommodate frictional forces and facilitate grain-to-grain sliding, as the phyllosilicates create multiple weak planes within the fault gouge.

This leads to stable sliding behaviour, which, when combined with a lower co-efficient of friction, promotes fault creep (Scott *et al.,* 2020). From Figures 18 a and b, it can be seen that the East Java Mud Volcano Complex, or Surabaya Mud Complex, or Kendeng Mud Complex (Kalangayar, Gununganyar and Wringin Anom) has different source characteristic than the Central Java Mud Volcano Complex, or Rembang Mud Volcano Complex (Kesongo and Grobogan Mud Volcano Complex). This may, of course, contribute to the creeping behaviour of the Kendeng Fault Zone.

Laboratory experiments demonstrate that halides, such as sodium chloride (NaCl), deform plastically at room temperature (Davidge and Pratt, 1964; Sprackling, 1970; Argon *et al.,* 1972; Bourcier *et al.,* 2012; Thom and Goldsby, 2019). The addition of water accelerates the weakening of rock salt through recrystallisation. The formation of fractures in halide, quartz, or calcite rocks reduces diffusion distances, thereby increasing the rate of pressure solution.

Electrochemical interactions between quartz and clay further enhance pressure solution creep. For this process to occur, soluble minerals such as feldspar, calcite, quartz, and serpentine must be present alongside a reactive fluid phase. Fine-grained materials typically facilitate minimal distance in diffusive mass transfer. Soluble grains must avoid sealing together to maintain rapid diffusive paths along solution seams. Two mechanisms help prevent sealing: (1) the passive concentration of phyllosilicates due to the depletion of soluble minerals during pressure solution and (2) the growth of new phyllosilicates, such as smectite, illite, or kaolinite (Gratier *et al.,* 2013).

Phyllosilicate minerals become trapped around soluble grains, preventing sealing and enabling continued diffusive mass transfer. Thin section analysis reveals that most carbonate mud and other minerals, including tuff, have transformed into phyllosilicate minerals such as smectite and illite. The presence of halides, smectite/illite, and fluid can enhance pressure solution creep. These mechanisms significantly influence most mud volcanoes in Indonesia, especially those associated with faults, anticlines, and fractures.

SEM analysis revealed that smectite, along with other minerals such as halide and quartz, dominated the Gununganyar Mud Volcano sample (Figure 18). In contrast, the Kesongo Mud Volcano sample was primarily composed of halide. These minerals play a crucial role in fault creeping (Farghalli and Langdon, 1974; Barber *et al.,* 2010).

Thin-section and scanning electron microscopy (SEM) analyses confirm the macroscopic observations of phyllosilicate minerals on the surface. In the Gununganyar SEM samples (Figure 18), quartz and halide grains were surrounded by smectite minerals. This arrangement enhances solution creep pressure, thereby contributing to fault creeping. Further investigation is needed to explain the relationship between the creeping activity of the Kendeng Fault and the overpressure conditions surrounding it. Assessing well data and seismic lines will be advantageous in determining the subsurface nature of the Kendeng Fault Zone, providing valuable additional information to the surface geological data presented in this paper.

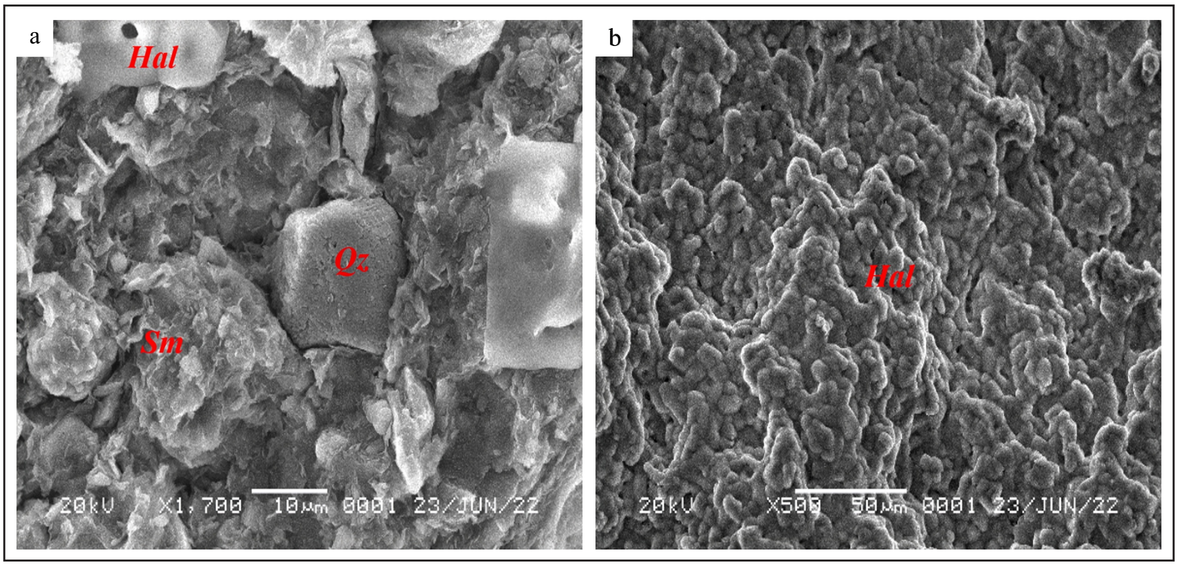

Figure 18. SEM of mud samples from Gununganyar (a) and Kesongo (b). *Hal*: Halide; *Qz*: Quartz; *Sm*: Smectite.

Conclusions

The surface geological mapping and laboratory analysis of samples lead to conclude that a creep mechanism is possible in the Kendeng Fault Zone. The Kendeng Fault Zone meets the three main criteria for creep: geology, fault geometry, and subsurface overpressure fluid. Marl dominates the lithology of the Kendeng Fault. Thin-section analysis classifies it as a mudstone abundant in carbonate mud that has transformed into clay minerals. This clay plays a key role in generating possible creep activity in the Kendeng Fault. On the other hand, SEM analysis confirms the presence of clay and halide minerals, which may also contribute to creep activity.

Manifestations of creep near fault planes are clearly visible through geological phenomena, such as landslides or physical changes in buildings. The Kendeng Fault geometry can be seen in its roughness in the studied area, indicating a slower creep rate than other creeping faults around the world, such as the Alto Tiberina, Chishang, and San Andreas Faults. The Central Java morphology (Grobogan area) is rougher than the East Java morphology (Surabaya area), suggesting a possible difference in creep rate.

The Central Java Fault segment has a higher creep rate than the East Java Fault segment. The focal mechanism of the recent earthquakes in the Kendeng Fault Zone suggests that the fault mechanism involved is a strike-slip or thrust fault. The two locations of the swarm of earthquakes in Gunung Pandan and Rawa Bening are evidence of fault creep in the western part of the Kendeng Fault Zone. This confirms that the western part of the Kendeng Fault Zone (Grobogan) experiences more active creep than the eastern part (Surabaya).

The elemental analysis results of the fluids and mud, combined with the gas analysis from all the mud volcanoes in the Java and Madura Islands, appear to align with the creeping rate differences and fault behaviour in Java, especially the onshore of the Northeast Java Basin. Correlation co-efficient (r) and determination (R^2) co-efficient analysis provide a detailed summary of the relationship between gas and fluid parameters from the mud volcanoes.

There is a positive correlation between the possible halide minerals (Na, Mg, Ca, K, and Cl) and the gas content (N_2 and O_2/Ar), with a slight relationship between these gases and fluid elements. Magnesium (Mg) and calcium (Ca) from the liquid sample are the most correlated with N_2 and O_2/Ar from the gas sample. These parameters increase from the mud volcanoes in East Java to those in Central Java.

The presence of halides and clay minerals was also confirmed by thin section and SEM analyses. These results suggest that the Grobogan and Kesongo Mud Volcano Complexes in Central Java are more strongly influenced by volcanic or tectonic activity than the Surabaya Mud Volcano Complex in East Java. Another indication that strengthens this point is the negative correlation between CO_2 and CH_4, which is supported by a high co-efficient of determination (R^2) indicating their relationship with each other.

The concentrations of CO_2 and CH_4 in the gas are negatively correlated (r), yet they are also connected (R^2). The Central Java Mud Volcanoes are primarily composed of CO_2, which may be a result of volcanic activity linked to tectonic processes in the region's deeper reservoir. In contrast, the East Java Mud Volcanoes are dominated by methane, which may result from a highly overpressurised hydrocarbon reservoir due to a high sedimentation rate.

This is also confirmed by the difference in sedimentation rates between East and Central Java. The dominant presence of halide minerals in fluids and gases may contribute to the creep rate and behaviour of the fault. The Kendeng Fault segment in Central Java appears to creep more actively than the East Java segment, as indicated by higher concentrations of halide minerals and CO_2 gas.

The East Java Mud Volcanoes are characterized by a very high content of methane (CH_4), which is suspected to originate from a hydrocarbon reservoir. Overpressure conditions, resulting from a very high sedimentation rate, influence the slow-creeping segment in East Java (the Surabaya region). Volcanism influence due to tectonics is less than that of the Kendeng Fault segment in Central Java (Grobogan region). This contributes to the difference in creep rates between East and Central Java, which may also contribute to the region's earthquake potential. The results also support the idea that the Kendeng Fault is segmented with different creep rates. These findings require further study, particularly the relationship of overpressure in each Kendeng Fault segment. This information will be useful for hydrocarbon exploration activities and natural disaster mitigation in the region. Future studies will be based on available wells and seismic data in the region to better understand the subsurface nature of the Kendeng Fault and its surroundings, which will add important value to this surface geological mapping.

References

Agostinetti, N.P., Licciardi, A., Piccinini, D., Mazzarini, F., Musemeci, G., Saccorotti, G., and Chiarabba, C. 2017. Discovering geothermal supercritical fluids: a new frontier for seismic exploration. *Scientific Reports,* 7 (14592), p.1-9. DOI: 10.1038/s41598-017-15118-w.

Amin, T.C., Ratman, N., and Gafoer, S., 1999. *Geological Map of Middle Part of Jawa, scale 1:500000*. Geological Research and Development Centre.

Anderlini, L., Serpelloni, E., and Belardinelli, M.E., 2016. Creep and locking of a low-angle normal fault: Insights from the Altotiberina fault in the Northern Apennines (Italy). *Geophysical Research Letters,* 43 (9), p.4321-4329. DOI: 10.1002/2016GL068604.

Argon, A.S., Nigam, A.K., and Padawer, G.E., 1972. Plastic deformation and strain hardening in pure NaCl at low temperatures. *Philosophical Magazine,* 25 (5), p.1095-1118. DOI: 10.1080/14786437208226855.

Avouac, J.P., 2015. From Geodetic Imaging of Seismic and Aseismic Fault Slip to Dynamic Modeling of the Seismic Cycle. *Annual Review of Earth and Planetary Sciences,* 43 (1), p.233-271. DOI: 10.1146/annurev-earth-060614-105302.

Baloglanov, E.E., Abbasov, O.R., and Akhundov, R.V., 2018. Mud volcanoes of the world: Classifications, activities and environmental hazard (informational-analytical review). *European Journal of Natural History,* 5, p.12-26.

Barber, D.J., Wenk, H.R., Hirth, G., and Kohlstedt, D.L., 2010. Dislocations in Minerals (2.10.2009). *Dislocation in Solids,* 16, p. 171-232. DOI: 10.1016/S1572-4859(09)01604-0.

Bemmelen, R.W. van, 1949. *The Geology of Indonesia*, V.F.A. Government Printing Office, The Hague, 732pp.

Blumetti, A.M., Grützner, C., Guerrieri, L., and Livio, F., 2017. Quaternary earthquakes: Geology and palaeoseismology for seismic hazard assessment, *Quaternary International,* 451. DOI: 10.1016/j.quaint.2017.04.002.

Bourcier, M., Dimanov, A., Héripré, E., Raphanel, J., Bornert, M., and Desbois, G., 2012. *Full field investigation of salt deformation at room temperature: cooperation of crystal plasticity and grain sliding. Mechanical Behaviour of Salt VII*. CRC Press, France.

Bürgmann, R., 2018. The geophysics, geology and mechanics of slow fault slip. *Earth and Planetary Science Letters,* 495, p.112-134. DOI: 10.1016/j.epsl.2018.04.062.

Burhannudinnur, M., 2013. Pengaruh Tektonik dan Laju Sedimentasi dalam Pembentukan Gunung Lumpur di Zona Kendeng dan Rembang Cekungan Jawa Timur. *Doctoral Program Dissertation*, Institut Teknologi Bandung. p.1-138.

Cabassi, J., Tassi, F., Vaselli, O., Fiebig, J., Nocentini, M., Capecchiacci, F., Rouwet, D., and Bicocchi, G., 2013. Biogeochemical processes involving dissolved CO_2 and CH4 at Albano, Averno, and Monticchio meromictic volcanic lakes (Central-Southern Italy). *Bulletin of Volcanology,* 75 (683). p.1-19. DOI:10.1007/s00445-012-0683-0.

Cakir, Z., S. Ergintav, S., Ozener, H., Dogan, U., Akoglu, A.M., Meghraoui, M., and Reilinger, R., 2012. Onset of aseismic creep on major strike-slip faults, *Geology,* 40, p.1115-1118. DOI: 10.1130/G33522.1.

Chao, H.C., You, C.F., Liu, H.C., and Chung, C.H., 2013. The origin and migration of mud volcano fluids in Taiwan: Evidence from hydrogen, oxygen, and strontium isotopic compositions. *Geochimica et Cosmochimica Acta,* 114, p.29-51. DOI: 10.1016/j.gca. 2013.03.035.

Chao, H.C., You, C.F., Lin, I.T., Lu, H.Y., Liu, H.C., and Chung, C.H., 2021. Water of eastern Taiwan mud volcanoes. Part I. H, triple O, triple Sr isotopes, and trace elements of Lo-Shan mud volcano. *Terrestrial, Atmospheric and Oceanic Sciences,* 32 (6.3), p.1227-1253,. DOI: 10.3319/TAO.2021.12.26.01.

Chao, H.C., 2023. Water of Eastern Taiwan mud volcanoes: part II-trace element distribution of Lei-Gong-Huo mud volcano. *Terrestrial, Atmospheric and Oceanic Sciences,* 34 (1), p.1-13. DOI: 10.1007/s44195-022-00033-z.

Chen, K.H. and Bürgmann, R., 2017. Creeping faults: good news, bad news? *Reviews of Geophysics,* 55 (2), p.282-286. DOI: 10.1002/2017RG000565.

Chen, Y., Chen, K.H., Hu, J., and Lee, J., 2020. Probing the Variation in Aseismic Slip Behaviour Around an Active Suture Zone: Observations of Repeating Earthquakes in Eastern Taiwan. *Journal of Geophysical Research: Solid Earth,* 125 (5), p.1-22. DOI: 10.1029/2019JB018561.

Chiaraluce, L., Amato, A., Carannante, S., Castelli, V., Cattaneo, M., Cocco, M., Collettini, C., D'Alema, E., Di Stefano, R., Latorre, D., Marzorati, S., Mirabella, F., Monachesi, G., Piccinini, D., Nardi, A., Piersanti, A., Stramondo, S., and Valoroso, L., 2014. The Alto Tiberina Near Fault Observatory (northern Apennines, Italy). *Annals of Geophysics,* 57 (3), p.1-16. DOI: 10.4401/ag-6426.

Chiodini, G., Cardellini, C., Di Luccio, F., Selva, J., Frondini, F., Caliro, S., Rosiello, A., Beddini, G., and Ventura, G., 2020. A correlation between tectonic CO_2 Earth degassing and seismicity is revealed by a 10-year record in the Apennines, Italy. *Science Advances,* 6 (35), p.1-7. DOI: 10.1126/sciadv.abc2938 eabc2938.

Davidge, R.W. and Pratt, P.L., 1964. Plastic Deformation and Work-Hardening in NaCl. *Physica Status Solidi B-Basic Solid-State Physics,* 6 (3), p.759-776. DOI: 10.1002/pssb.19640060315.

Dunham, R.J., 1962. Classification of Carbonate Rocks According to Depositional Texture. In: Ham, W.E. (ed.), *Classification of Carbonate Rocks*, AAPG, Tulsa.

Essing, D. and Poli, P., 2022. Spatiotemporal Evolution of the Seismicity in the Alto Tiberina Fault System Revealed by a High-Resolution Template Matching Catalogue. *Journal of Geophysical Research: Solid Earth,* 127 (10), p.1-17. DOI: 10.1029/2022JB024845.

Farghalli, A. M. and Langdon, T.G., 1974. Method of estimating stacking fault energies in alkali halide crystals using creep data. *Journal Applied Physics,* 45 (5), p.1965-1967. DOI: 10.1063/1.1663531.

Franklin, K.R. and Huang, M., 2022. Revealing Crustal Deformation and Strain Rate in Taiwan Using InSAR and GNSS. *Geophysical Research Letters,* 49 (21), p.1-10. DOI: 10.1029/2022GL101306.

Gafoer, S. and Ratman, N., 1999. *Geological Map of Eastern Part of Jawa, scale 1:500000*. Geological Research and Development Centre.

Gori, S., Falcucci, E., Kayen, R.E., Zimmaro, P., Lingwall, B., Galadini, F., and Stewart, J.P., 2018. Surface fault rupture from 2016 Central Italy Earthquake Sequence. *Proceedings, 11th National Conference in Earthquake Engineering,* Los Angeles.

Gratier, J.P., Renard, F., and Labaume, P., 1999. How pressure solution creep and fracturing processes interact in the upper crust to make it behave in both a brittle and viscous manner. *Journal of Structural Geology,* 21 (8-9), p.1189-1197. DOI: 10.1016/S0191-8141(99)00035-8.

Gratier, J.P., Dysthe, D., and Renard, F., 2013. The role of pressure solution creep in the ductility of the Earth's upper crust. *Advances in Geophysics,* 54, p.47-179. DOI: 10.1016/B978-0-12-380940-7.00002-0.

Hadizadeh, J., Boyle, A.P., Andrea E., and Gaughan, A.E., 2024. A study of fluid overpressure microstructures from the creeping segment of the San Andreas fault. *Journal of Structural Geology,* 180 (105065), p.1-15. DOI: 10.1016/j.jsg.2024.105065.

Harianto, S., 2018. *Semburan Air Campur Lumpur di Ngawi Sangat Kuat, Ini Buktinya*. https://news.detik.com/berita-jawa-timur/d-4150982/semburan-air-campur-lumpur-di-ngawi-sangat-kuat-ini-buktinya [27 August, 2025].

Harris, R.A., 2017. Large earthquakes and creeping faults. *Reviews of Geophysics,* 55 (1), p.169-198. DOI: 10.1002/2016RG000539.

Herwegh, M., Xiao, X., and Evans, B., 2003. The effect of dissolved magnesium on diffusion creep in calcite. *Earth and Planetary Science Letters,* 212 (3-4), p.457-470. DOI: 10.1016/S0012-821X(03)00284-X.

Hirao, B., Savage, H., and Brodsky, E.E., 2021. Communication Between the Northern and Southern Central San Andreas Fault via Dynamically Triggered Creep. *Geophysical Research Letters,* 48 (13), p.1-10. DOI: 10.1029/2021GL092530.

Humaida, H., Zaenuddin, A., and Sutaningsih, N.E., 2012. Semburan gas bercampur air di desa candi Pari, Kecamatan Porong, Kabupaten Sidoarjo, Jawa Timur. *Jurnal Lingkungan dan Bencana Geologi,* 3 (1), p.1-19. DOI:10.34126/JLBG.V3I1.32.

Jolivet, R., Simons, M., Agram, P.S., Duputel, Z., and Shen, Z.K., 2015. Aseismic slip and seismogenic coupling along the central San Andreas Fault. *Geophysical Research Letters,* 42 (2), p.297-306. DOI: 10.1002/2014GL062222.

Julias, R.N., Muslih, Y.B., Agatra, G., Nugraha, A., Ramadhan, T., and Husein, S., 2017. Surface Evidences on Understanding Paleogene Structure between Kendeng Basin with East Java Basin and Southern Mountain. *Proceedings, HAGI-IAGI-IAFMI-IATMI Joint Convention Malang.*

Khoshmanesh, M. and Shirzaei, M., 2018. Episodic creep events on the San Andreas Fault caused by pore pressure variations. *Nature Geoscience,* 11 (8), p.610-614. DOI: 10.1038/s41561-018-0160-2.

Kim, W., Hong, T.K., Lee, J., and Taira, T., 2016. Seismicity and fault geometry of the San Andreas fault around Parkfield, California and their implications. *Tectonophysics,* 677-678, p.34-44. DOI: 10.1016/j.tecto.2016.03.038.

Koulali, A., Susilo, S., Mcclusky, S., Meilano, I., Cummins, P., Tregoning, P., Lister, G., Efendi, J., and Syafi'i, M.A., 2016. Crustal strain partitioning and the associated earthquake hazard in the eastern Sunda-Banda Arc. *Geophysical Research Letters,* 43, p.1943-1949. DOI: 10.1002/2016GL067941.

Lee, J., Angelier, J., Chu, H., Hu, J., Jeng, F., and Rau, R., 2003. Active fault creep variations at Chihshang, Taiwan, revealed by creep meter monitoring, 1998-2001. *Journal of Geophysical Research: Solid Earth,* 108 (B11), p.1-21. DOI: 10.1029/2003JB002394.

Lee, S.J., Liu, T.Y., and Lin, T.C. 2023. The role of the west-dipping collision boundary fault in the Taiwan 2022 Chihshang earthquake sequence. *Scientific Reports* 13 (1), 3552p. DOI: 10.1038/s41598-023-30361-0.

Lestari, W., Widodo, A., Syaifuddin, F., and Warnana, D.D., 2020. Research priority of the potential earthquake on the Java Island using decision-making analysis. *E3S Web of Conferences* 156, p.1-5. DOI: 10.1051/e3sconf/202015603003.

Ma, X., Zhou, Y., Dang, J., Zhang, L., and He, C., 2024. Mineralogical and frictional properties of fault rocks from the Laohushan creep segment of the Haiyuan fault, Northeastern Tibet, *Journal of Structural Geology,* 178, p.1-17. DOI: 10.1016/j.jsg.2023.105017.

Marshall, N., Kazimova, S., Kazimova, I., Pierce, I., Johnson, B., Walker, R., Rhodes, E., and De Pascale, G. 2024. Paleosesimology of West Caspian Fault (Azerbaizan) and active faulting in an over-pressured sedimentary basin. *Proceedings, 12th International INQUA*

Meeting on Paleoseismology, Active Tectonic and Archaeoseismology. Los Andes.

Mazzini, A., Etiope, G., and Svensen, H., 2012. A new hydrothermal scenario for the 2006 Lusi eruption, Indonesia. Insights from gas geochemistry. *Earth and Planetary Science Letters,* 317-318, p.305-318. DOI: 10.1016/j.epsl.2011.11.016.

Miller, S.A. and Mazzini, A., 2018. More than ten years of Lusi: A review of facts, coincidences, and past and future studies. *Marine and Petroleum Geology,* 90, p.10-25. DOI: 10.1016/j.marpetgeo.2017.06.019.

Moore, D.E. and Rymer, M.J., 2007. Talc-bearing serpentinite and the creeping section of the San Andreas fault. *Nature,* 448 (7155), p.795-797. DOI: 10.1038/nature06064.

Navarro, J.S., Stix, J., and De Moor, J.M., 2022. A new multi-GAS system for continuous monitoring of CO2/ CH4 ratios at active volcanoes. *Journal of Volcanology and Geothermal Research,* 426 (107533), p.1-12. DOI: 10.1016/j.jvolgeores.2022.107533.

Noya, Y., Suwarti, T., Suharsono, and Sarmili, L., 1992. *Geological Map of The Mojokerto Quadrangle, Jawa, scale 1:100000*. Geological Research and Development Centre.

Ougier-Simonin, A. and Zhu, W., 2013. Effects of pore fluid pressure on slip behaviours: An experimental study. *Geophysical Research Letters,* 40 (11), p.2619-2624. DOI: 10.1002/grl.50543.

Prasetyadi, C., Suparka, E.R., Harsolumakso, A.H., and Sapiie, B., 2005. Eastern Java basement rock study: preliminary results of recent field study in Karangsambung and Bayat areas. *Proceedings, The 34th Annual Convention of the Association of Indonesian Geologists,* Surabaya.

Pringgoprawiro, H., 1983. Biostratigraphy and Paleogeography of the North-East Java Basin, A New Approach, Doctoral Dissertation, Bandung Institute of Technology.

Pringgoprawiro, H. and Sukido, 2011. *Geological Map of The Bojonegoro Quadrangle, East Jawa, scale 1:100000.* Centre for Geological Survey.

Putriyana, L., Daud, Y., Aziz, M., Nasruddin, N., and Hesty, N., 2023. *Evaluation and ranking of the CO2 storage potential in low to medium temperature geothermal fields in Indonesia. Case Studies in Chemical and Environmental Engineering,* 8, p.1-9. DOI: 10.1016/j.cscee.2023.100406.

Rainone, M.L., Rusi, S., and Torrese, P., 2015. Mud volcanoes in central Italy: Subsoil characterization through a multidisciplinary approach. *Geomorphology,* 234, p.228-242. DOI: 10.1016/j.geomorph.2015.01.026.

Ramdhan, A.M., Hakim, F., Hutasoit, L.M., Goulty, N.R., Sadirsan, W., Arifin, F., Endarmoyo, K., Firmansyah, R., Zainal, R.M., Gulo, M.Y., SihmN, m., Suseno, P.H., and Purwanto, A.H., 2013. Importance of Understanding Geology in Overpressure Prediction: The Example of The East Java Basin. *Proceedings, 37th Annual Convention and Exhibition, Indonesian Petroleum Association, Jakarta.*

Rofiq, A., 2021. *Ada Dua Dugaan Penyebab Sumur Bor di Bojonegoro Semburkan Air 15 Meter.* https://news.detik.com/berita-jawa-timur/d-5698661/ada-dua-dugaan-penyebab-sumur-bor-di-bojonegoro-semburkan-air-15-meter [27 August, 2025].

Rymer, M.J., Hickman, S.H., and Stoffer, P.W., 2006. A field guide to the central, creeping section of the San Andreas fault and the San Andreas Fault Observatory at Depth. In: Prentice, C.S., Scotchmoor, J.G., Moores, E.M., and Kiland, J.P. (eds.) GSA Field Guide 7: 1906 *San Francisco Earthquake GSA Field Guides*. Geological Society of America, America. p.237-272. DOI: 10.1130/2006.1906SF(16).

Saffer, D.M., Lockner, D.A., and Mckiernan, A., 2012. Effects of smectite to illite transformation on the frictional strength and sliding stability of intact marine mudstones, *Geophysical Research Letters,* 39 (L11304), p.1- 6. DOI:10.1029/2012GL051761.

Santoso, D., Wahyudi, E.J., Kadir, W.G.A., Alawiyah, S., Nugraha, A.D., Supendi, P., and Parnadi, W.W., 2018. Gravity Structure around Mt. Pandan, Madiun, East Java, Indonesia and Its Relationship to 2016 Seismic Activity. *Open Geosciences,* 10 (1), p.882-888. DOI: 10.1515/geo-2018-0069.

Scholz, C., 2019. *The Mechanics of Earthquakes and Faulting. 3rd ed*. Cambridge University Press, Cambridge. 517pp.

Schultz, R., Skoumal, R. J., Brudzinski, M. R., Eaton, D., Baptie, B., and Ellsworth, W., 2020. Hydraulic fracturing-induced seismicity. *Reviews of Geophysics,* 58, p.1-43. DOI: 10.1029/2019RG000695.

Scott, C., Bunds, M., Shirzaei, M., and Toke, N., 2020. Creep Along the Central San Andreas Fault from Surface Fractures, Topographic Differencing, and InSAR. *Journal of Geophysical Research: Solid Earth,* 125 (10), p.1-16. DOI: 10.1029/2020JB019762.

Shirzaei, M., Rudolph, M.L., and Manga, M., 2015. Deep and shallow sources for the Lusi mud eruption revealed by surface deformation, *Geophysical Research Letter,* 42, p.5274-5281. DOI:10.1002/2015GL064576.

Sibson, R.H., 2014. Earthquake rupturing in fluid-overpressured crust: How common? *Pure Applied Geophysics,* 171 (11), p.2867-2885. DOI: 10.1007/s00024-014-0838-3.

Sitinjak, E.S., 2016. Analysis of the relationship between wellbore stability and overpressure zone in Tanggulangin area, Norteast Java Basin. *Master Thesis at Dept. of Geology, Faculty of Earth Science and Technology*, Bandung Institute of Technology, p.91-94.

Sitinjak, E.S., Sapiie, B., Ramdhan, A.M., Harianto, M., Somantri, W., Nurcahyo, M., and Juriansyah, M., 2017. Implication of Overpressure Zone to Wellbore Stability for Field Development in Onshore Northeast Java Basin. *Proceedings of HAGI - IAGI - IAFMI-IATMI Joint Convention Malang (JCM 2017), 25th-28th September 2017, Malang*, Indonesia.

Sitinjak, E., 2018. The Overpressure Mechanism Identification in Unstable Shale Environment. *Conference, AAPG/EAGE/MGS 4th Myanmar Oil and Gas Conference, Yangoon*.

Sitinjak, E.S. and Harbowo, D.G., 2024. Mud Volcanoes and Adjacent Vegetation Adaptation in the Rembang Zone, Indonesia: An Approach for Mud Volcano Investigation. *IOP Conference Series: Earth and Environmental Science,* 1373 (012029), p.1-17. DOI: 10.1088/1755-1315/1373/1/012029.

Smyth, H., Hall, R., and Nichols, G.J., 2005. East Java: Cenozoic Basins, Volcanoes and Ancient Basement. *Proceedings of 30th Annual and Exhibition of Indonesian Petroleum Association. Jakarta.*

Smyth, H., Hall, R., Hamilton, J., and Kinny, P., 2008. Cenozoic Volcanic Arch Hystory of East Java, Indonesia: The Stratigraphic Record of Eruptions on An Active Continental Margin. *The Geological Society of America,* 436, p.199-222. DOI: 10.1130/2008.2436(10).

Sprackling, M.T., 1970. The plastic bending of NaCl. The Philosophical Magazine: *A Journal of Theoretical Experimental and Applied Physics,* 21 (173), p.913-921. DOI: 10.1080/14786437008238480.

Steinbrugge, K.V., Zacher, E.G., Tocher, D., Whitten, C.A., and Claire, C.N. 1960. Creep on the San Andreas Fault. *Bulletin of the Seismological Society of America* 50 (3), p.389-415. DOI: 10.1785/BSSA0500030389.

Sukardi and Budhitrisna, T., 1992. *Geological Map of The Salatigao Quadrangle, Jawa, 1:100000*. Geological Research and Development Centre.

Thom, C.A. and Goldsby, D.L., 2019. Nanoindentation Studies of Plasticity and Dislocation Creep in Halite. *Geosciences,* 9 (2), 79p. DOI: 10.3390/geosciences9020079.

Thomas, M.Y., Avouac, J.P., Gratier, J.P., and Lee, J.C., 2014. Lithological control on the deformation mechanism and the mode of fault slip on the Longitudinal Valley Fault, Taiwan. *Tectonophysics,* 632, p.48-63. DOI: 10.1016/j.tecto.2014.05.038.

Tong, X., Sandwell, D.T., and Smith-Konter, B., 2013. High-resolution interseismic velocity data along the San Andreas Fault from GPS and InSAR. *Journal of Geophysical Research: Solid Earth* 118 (1), p.369-389. DOI: 10.1029/2012JB009442.

Valoroso, L., Chiaraluce, L., Di Stefano, R., and Monachesi, G., 2017. Mixed-Mode Slip Behaviour of the Altotiberina Low-Angle Normal Fault System (Northern Apennines, Italy) through High-Resolution Earthquake Locations and Repeating Events. *Journal of Geophysical Research: Solid Earth,* 122 (12), p. 10220-10240. DOI: 10.1002/2017JB014607.

Watt, J.T., Ponce, D.A., Graymer, R.W., Jachens, R.C., and Simpson, R.W., 2014. Subsurface geometry of the San Andreas-Calaveras fault junction: Influence of serpentinite and the Coast Range Ophiolite. *Tectonics* 33 (10), p.2025-2044. DOI: 10.1002/2014TC003561.

Wei, M., Sandwell, D., and Fialko, Y., 2009. A silent M w 4.7 slip event of October 2006 on the Superstition Hills fault, southern California. *Journal of Geophysical Research: Solid Earth,* 114 (B7). DOI: 10.1029/2008JB006135.

Xu, X., Ward, L., Jiang, J., Smith-Konter, B., Tymofyeyeva, E., Lindsey, E.O., Sylvester, A.G., and Sandwell, D.T., 2018. Surface creep rate of the southern San Andreas fault modulated by stress perturbations from nearby large events. *Geophysical Research Letters,* 45, p.10259-10268. DOI: 0.1029/2018GL080137.

Xu, X., Sandwell, D.T., Klein, E., and Bock, Y., 2021. Integrated Sentinel-1 InSAR and GNSS Time-Series Along the San Andreas Fault System. *Journal of Geophysical Research: Solid Earth,* 126 (11), p.1-15. DOI: 10.1029/2021JB022579.

Zaennudin, A., Humaida, H., Saing, U.B., and Laksono, R.W., 2013. Semburan gas bercampur air dan lumpur di Desa Metatu, Kecamatan Benjeng, Kabupaten Gresik, Jawa Timur. *Jurnal Lingkungan dan Bencana Geologi*, 4 (3), p.179-197.